



***Facultad  
de  
Ciencias***

**Estudio de variabilidad estelar mediante  
adquisición y análisis de observaciones  
astronómicas.**

**(Stellar variability study through acquisition  
and analysis of astronomical observations.)**

Trabajo de Fin de Grado  
para acceder al

**GRADO EN FÍSICA**

**Autor: Marta Rosas Mediavilla**

**Director: Amalia Corral Ramos**

**02 - 2022**

# Contents

<b>1</b>	<b>Introduction</b>	<b>4</b>
1.1	Stellar evolution . . . . .	4
1.1.1	Low to medium mass stars . . . . .	7
1.1.2	High mass stars . . . . .	8
1.2	Variable stars . . . . .	9
1.3	Light curves. Flux and magnitudes . . . . .	11
<b>2</b>	<b>Methods</b>	<b>14</b>
2.1	Image acquisition. Astronomical observations . . . . .	14
2.1.1	Visibility . . . . .	14
2.1.2	Instrumentation . . . . .	16
2.2	Image reduction . . . . .	17
2.2.1	Software for image reduction . . . . .	19
2.3	Image analysis: photometry and differential photometry . . . . .	20
2.4	Data analysis: light curve . . . . .	24
2.4.1	Variability detection . . . . .	24
2.4.2	Variability characterization: Fourier analysis . . . . .	25
2.4.3	Software for data analysis . . . . .	27
<b>3</b>	<b>Results</b>	<b>29</b>
3.1	Observations . . . . .	29
3.2	Reduction . . . . .	30
3.3	Light curve extraction . . . . .	32
3.3.1	Choosing comparison stars . . . . .	32
3.3.2	Differential photometry . . . . .	35
3.3.3	Variability detection . . . . .	37
3.4	Light curve analysis . . . . .	39
<b>4</b>	<b>Discussion</b>	<b>46</b>
<b>5</b>	<b>Conclusions</b>	<b>48</b>
<b>6</b>	<b>Bibliography</b>	<b>48</b>

### Abstract

The aim of this project was to work with actual astronomical images obtained from the Observatorio Astronómico de Cantabria to study a variable star. A variable star is a star whose brightness changes overtime.

To achieve this, it was necessary to learn how to work with real astronomical data and how to remove instrumental effects as much as possible through the process of image reduction to optimize the results. From the reduced images the light curve of the target star was obtained.

The light curve, which is the representation of the variation in brightness (flux or magnitude) along time, contains important information about the star. Through the analysis of this information, it was determined that the star observed displays periodic variability, and has a main period of  $P=0.095$  days.

Due to this short period, the shape of its light curve, and the amplitude of the variation in magnitude/flux, it was concluded that the target star belongs to the group of  $\delta$  Scuti stars, more specifically, High-Amplitude  $\delta$  Scuti stars (HADS). This stars are at the end of their hydrogen burning stage so they are about to end their main sequence stage and enter the giant phase.

**Key words:** astronomical data, star, variable star,  $\delta$  Scuti, image reduction, light curve.

### Resumen

El objetivo de este proyecto es trabajar con imágenes astronómicas reales obtenidas desde el Observatorio Astronómico de Cantabria para estudiar una estrella variable. Una estrella variable es una estrella cuya luminosidad cambia a lo largo del tiempo.

Para lograr esto, fue necesario aprender a trabajar con datos astronómicos reales, cómo los errores sistemáticos funcionan y cómo compensarlos lo máximo posible mediante el proceso de reducción de imágenes para optimizar los resultados obtenidos. A partir de estas imágenes reducidas se obtiene la curva de luz de la estrella.

La curva de luz, que es la representación de la variación de luminosidad (flujo o magnitud) a lo largo del tiempo, contiene información importante sobre la estrella. Mediante el análisis de esta información, se determinó que la estrella observada muestra una variabilidad periódica y su periodo principal es de  $P=0.095$  días.

Debido a este periodo tan corto, la forma de la curva de luz y la amplitud de la variación en flujo o magnitud, se concluye que la estrella observada pertenece al grupo de estrellas  $\delta$  Scuti. Específicamente, pertenece a las  $\delta$  Scuti de alta amplitud (HADS). Este tipo de estrellas normalmente están experimentando el final de su fase en la secuencia principal debido a que se están quedando sin hidrógeno como combustible, y a punto de entrar en la fase de estrellas gigantes.

**Palabras clave:** datos astronómicos, estrella, estrella variable,  $\delta$  Scuti, reducción de imágenes, curva de luz.

# 1 Introduction

## 1.1 Stellar evolution

Stars are big masses of gas that emit light due to their internal process of nuclear fusion. They may appear to have constant magnitudes or brightness, and some may keep a constant magnitude for millions of years. However, the changes in their chemical composition due to the processes of nuclear fusion make any star go through a journey changing its mass and brightness overtime as it evolves.

There are some important stages in the evolution of a star, which can be represented in the HR diagram. The Hertzsprung-Russell diagram, HR diagram for short, is a diagram used to show the different types of stars, but it also can show their evolution. A representation of this diagram is shown in figure 1. It is usually a representation of the luminosity as a function of the spectral class. The spectral class is related to the temperature of the star, the further into the right we go into the diagram, the cooler the star will be. On the other axis, the luminosity not only represents how bright the star is. If a star is in the same spectral class (has the same temperature) than other star, but one is much brighter than the other, this means that the brighter star must have a bigger surface area, meaning that the brighter the star the bigger it is. To sum up, this diagram does not only give information about the spectral class of the star and its luminosity, but also about its temperature and the mass of the star.

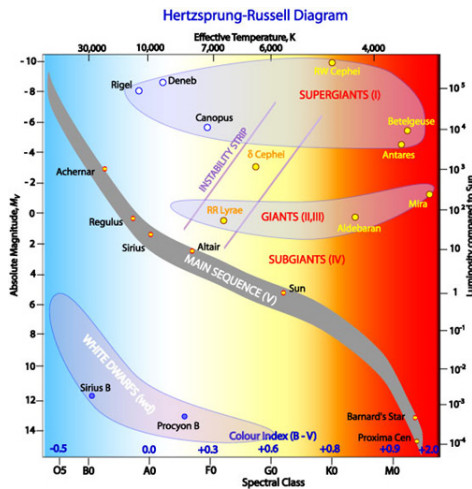


Figure 1: HR diagram showing the main types of stars and their evolutionary stages. (1)

Some types of stars in the diagram are named. These represent the different stages of a star's life. The main sequence is this line that goes across the diagram and is the most stable so it is the most populated part of the diagram. The giant and supergiant reds are on top, being quite an unstable part of the process

and finally the last notable group are the white dwarfs at the bottom left, that are also known as dying stars.

Stars will move across this diagram during their life, although most of their time will be spent on the main sequence. They enter the main sequence at different points depending on the initial mass as shown in figure 2. Then, they will stay on the main sequence, moving slightly to the left until they get to a point where they enter what's called the giant branch and will move away from the main sequence as shown in figure 3.

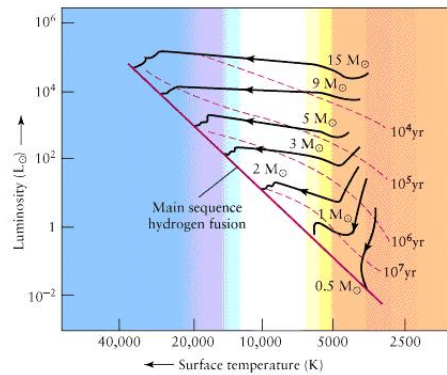


Figure 2: HR diagram showing the path of some stars with different masses entering the main sequence. Figure extracted from (2)

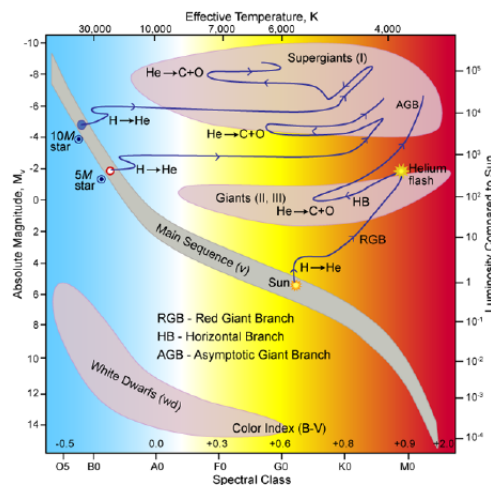


Figure 3: HR diagram showing the path of some stars with different masses leaving the main sequence. Figure extracted from: (3)

Star evolution begins with what is called a protostar, which are formed

when a big cloud of gas is in a process of contraction. When it contracts, its gravitational potential energy is liberated and transforms mostly into radiation. At first, as the density is low, these radiation can move freely and temperature does not increase a considerable amount. Nonetheless, as the gas cloud contracts and the density and pressure increase in the centre, radiation can no longer travel freely so most of the energy is converted into heat, rising the temperature of the centre of the cloud, which also contributes to a growth on pressure. The contraction of the centre eventually slows down and, at this stage, it is considered a protostar. This contraction will stop when the protostar reaches hydrostatic equilibrium. This means that the force of gravity trying to contract the gas is equal to the force induce by the reactions on the core. Protostars are mainly composed by hydrogen molecules, that will eventually ionise. They are located inside a mass of gas, so they are adding material and growing its mass steadily.

The protostar is quite cool and faint in the beginning so it sits in the bottom right of the HR diagram. It will evolve and, as it collapses and the temperature raises, it will move upwards. When the temperature on the nucleus becomes high enough for fusion to take place between the hydrogen atoms to form helium, the protostar is considered a proper star. It will move upwards and to the left of the HR diagram. The star will sit within the main sequence around the same place and, depending on the initial mass of gas that formed the star, it will be situated towards the left (bigger mass) or the right (lower mass). More massive stars get to this main sequence stage earlier than smaller ones as their bigger mass implicates that their core temperature will be higher and nuclear fusion will be able to occur sooner. Because of this, the protostar phase can last for just a few thousand of years in more massive stars to several hundreds of millions of years if the star is less massive.

A star is on the main sequence phase when all of its energy is produced by the fusion of hydrogen atoms. At this stage the star is considered very stable, with changes only occurring because its chemical composition is gradually changing due to the nuclear reactions. This is the longest phase in every star's life. However, it is longer for smaller stars, as more massive stars radiate more energy thus consuming the hydrogen faster. As is the longest phase, it is more likely to find stars in this phase, so the HR diagram is very populated along the main sequence, mostly on the right part, as these less massive stars last longer in this phase.

The main sequence is usually divided in two segments, the upper main sequence, located on the left, where more massive stars are, and the lower main sequence, located at the right, where less massive stars are. To differentiate between them, the limit is set roughly at 1.5 solar masses (4).

Stars on the upper main sequence follow a different path than the ones on the lower one, both types of stars will eventually consume their hydrogen fuel, but they will behave differently. The upper main sequence stars will shift to the upper right of the HR diagram because their temperature will decrease but they will keep being really bright. On the other hand, on the lower main sequence stars the temperature is lower to begin with. The star will slowly move upwards

almost following the main sequence, becoming brighter and hotter, but with no big changes on the radius.

The main sequence phase is considered to end for both types of stars when they burn all the hydrogen on the centre. They enter what is called the giant phase. The lower main sequence stars will have a gradual and slow shift into giants whereas the upper ones will have a quicker transition.

### 1.1.1 Low to medium mass stars

Low to medium mass stars will start experiencing changes when the hydrogen starts to run out. As the radiation emitted by the core is lowering the force of gravity will make the core smaller. The remaining hydrogen will then start to fuse faster, liberating more radiation and provoking a rapid expansion of the outer layers of the star. This expansion means that the surface temperature of the star will reduce because it is further away from the core, making the star cooler on the surface even if the core is hotter. At this stage the star will be considered a red giant. During this process they will move almost horizontally towards the right of the HR diagram through the red giant branch. This stage may last for around a billion years. As hydrogen runs out, the core will keep shrinking getting smaller and hotter, until it experiences what's called a helium flash (4). This helium flash will happen when the core of the star reaches enough temperature to start the process of helium fusion, in a reaction that will transform helium in heavier metals such as carbon.

This is a new fuel that the star possesses now, and the star will enter what's called the asymptotic giant branch. This stage is quite unstable, the helium flash produces a disequilibrium on the hydrostatic equilibrium of the star, so, the star usually starts pulsating. This means that their radius changes in size while helium is being consumed. It will be explained in Sect. 1.2 that this changes in radius greatly affect the luminosity of the star, so the pulsation is not only a physical radius change but also a luminosity change. This pulsation will lead to the star getting progressively smaller in size. The temperature will rise until the helium that was used as fuel is running out and most of its core is heavier metals. The star runs out of enough material to keep the reaction going so it collapses. This means that the outer layers will start growing rapidly becoming a giant star again. However this time the star will start losing the outer layers of gas that remain as the last bursts of energy will eject it towards space, and it eventually may contribute to the creation of other stars.

The very hot core is left behind which will keep shrinking slightly reaching radius below earth's. But, with no material to burn, it slowly starts cooling down. This core is known as a white dwarf star. The cooling time of these stars is so long that some say it is comparable to the age of the universe and they have been used to set a lower limit to the age of the universe. White dwarfs have a mass lower than the Chandrasekhar mass, 1.4 solar masses (4), if it were to be above that mass it would be considered a neutron star, that will be discussed further in this section.

### 1.1.2 High mass stars

Going back to the high mass stars, they evolve differently as mentioned before. These stars have higher temperatures than the other stars, which leads to faster fusion of the hydrogen, thus running out earlier. As the other stars, when hydrogen starts to run out, the core will contract and rise its temperature, producing an expansion of the outer layers so it becomes a giant. However, the main difference is that the core temperature of these stars will not only allow for helium fusion but it will also allow heavier metals to go through a fusion reaction. They can produce carbon, oxygen, neon and even silicon. These materials form layers on the core, with heavier elements getting a smaller and smaller region of the core each time. This implicates that, as the core is smaller, the temperatures will get higher and the fusion of heavier elements will be possible. The heaviest element that has been found in the core of one of these stars is iron, as these nuclei are so stable that further fusion would not lead to any more energy released. Each layer of the core will keep undergoing their own reactions releasing energy with the iron in the centre, until there is no more fuel.

The outer layers of these stars expand much more than the giant as the radiation energy emitted from them is much higher, so they are usually referred to as supergiants. Supergiants usually have a great mass and they are really bright but have a low surface temperature as the outer layers are so far away from the core.

Once all the fuel is gone, the star experiences a sudden collapse that leads to the star exploding. This explosion ejects the outer layers and most of the heavier elements into space. This event is called a supernova and great amount of energy are liberated to space. Depending on how massive the star was there are two possible outcomes.

When the star collapses and it is not able to withstand the force of gravity. The core will collapse as explained before with such energy that all of the electrons would be able to react with the protons of their atom's nuclei transforming into neutrons. If the core of the star has a mass lower than 3 solar masses but higher than the Chandrasekhar mass, this reaction leaves behind a neutron star, called like that because is entirely formed by neutrons that act as if they were a huge atomic nuclei. However, if the core of the star had a mass higher than 3 solar masses, the force of gravity will be so high that the neutrons would not be able to stand it and they would collapse producing a black hole.

To sum up, stars experience different life cycles depending on their initial mass. They all begin as clouds of gas, that form a protostar that eventually becomes a proper star on the main sequence. If their mass is high enough they will become supergiants in their giant phase, but less massive stars will become just giants. Is during this giant phase that stars are more unstable and more likely to pulsate and vary its radius, which, as will be explained in Sect. 1.2, its related to its brightness. The stars will eventually become white dwarfs, neutron stars or black holes depending on their initial masses.

## 1.2 Variable stars

Although strictly all stars have variable brightness because they change their magnitude values overtime, some stars can have rapid changes in brightness and some of them pulsate in regular intervals, which means they have a period.

These variable stars are usually classified based on the shape of their light curve. A light curve is obtained by measuring the flux or brightness of the star along time and plotting the results, more information about light curves is discussed in Sect 1.3. If the star has a period, the light curve can be represented as a function of the phase associated with that period. Obtaining this light curve is the main objective of this project as it allows to classify and obtain a lot of information about the variable star.

There are three main types of variable stars: eruptive, eclipsing variables and pulsating. Eruptive stars are the ones that do not have regular periods, but sudden outbursts of matter are jetted into space. This eruption is what causes the changes in brightness. Eclipsing stars usually belong to a binary system of stars, in which the two components pass periodically one in front of the other from our perspective, thus producing changes on their brightness. So their changes in brightness are not due to physical changes within the star.

The third type, which will be the main focus of the project, are pulsating stars. The brightness of these stars follows a cycle, which means they have a period. The period of pulsation is related to a proper frequency which is the fundamental frequency of vibration of the star. Usually stars will have multiple frequencies at which they vibrate known as modes of vibration. The variation in brightness can be understood as a superposition of these modes.

More often than not, stars are stable, the gravity force attracting the gas towards the interior of the star is balanced by the reactions of the hot gas in the interior of the star. As explained in Sect. 1.1 this is the hydrostatic equilibrium in which stars usually are. This means that if a star starts to expand or contract the forces within it will lead it to reach this equilibrium.

Pulsating stars usually change its brightness because their radius changes as well. The change in radius induces changes in the wavelengths of their spectral lines (due to Doppler effect) and also some variation on the surface temperature. As the radius expands the density of gas within the star decreases, leading to a decrease on temperature and pressure. When the pressure is small enough the force of gravity is able to compress the gas again, reducing the radius of the star once again. The changes in temperature are the main cause of the observed changes on the star's brightness, as the luminosity,  $L$ , directly correlates with the effective temperature,  $T_e$ , as  $L \sim R^2 T_e^4$ . A change in the effective temperature is really noticeable on the star's luminosity, so indeed the luminosity and the radius of the star are strictly correlated.

For this process to be able to happen constantly so the star does not reach an hydrostatic equilibrium, there needs to be an internal mechanism allowing this changes in radius. This mechanism is the thermodynamic effect of an ionization zone in a star. This happens in stars where Helium has not totally ionize, it has only lost one of its electrons. When the star contracts, the interior heats slightly

and the helium fully ionizes. This requires energy, so this process is 'storing' energy in the form of ionization energy. As the star starts to expand due to the pressure of the gas, this stored energy gets liberated as helium atoms recombine with the electrons once lost. This gives the pulsating star an extra push of energy that lets it keep pulsating instead of reaching an equilibrium. Most of the stars that make use of this type of mechanism are located in what's called the instability strip in the HR diagram (figure 4). This includes different types of pulsating stars such as Cepheids, W Virgins, RR Lyrae,  $\delta$  Scuti and dwarf Cepheids.

One of the most important types of pulsating stars are the Cepheids. They are supergiants of spectral class F-K, with periods varying from 1 to 50 days and changes in the magnitude's amplitude range from 0.1 to 2.5. The form of their light curve usually shows a rapid increase in brightness followed by a slower decrease, in rapid regular periods. The luminosity of Cepheids is related to its period, because as mentioned before, changes in the radius, or the size of the star, are related to the luminosity variations. For Cepheids, the relation between the logarithm of period,  $\log P$ , and the absolute magnitude,  $M$ , is linear. This means that the analysis of their periods can be used to determine distances. This will be discussed in Sect. 2.2.

Other types of pulsating stars include W Virginis stars, which are similar to Cepheids but 1.5 magnitudes fainter for a determined period, RR Lyrae stars, whose magnitude variation is much smaller than Cepheids and so are their periods, and Mira Variables also known as long period variables, which have really long periods (100-500 days). All these pulsating stars have a regular period, but there are other types that may have semiregular or irregular periods. These irregular stars usually are young massive stars whose pulsations are unsteady but the mechanisms of this pulsations are not totally understood yet.

All these types of pulsating stars can be classified through the Cepheid instability strip in the HR diagram.

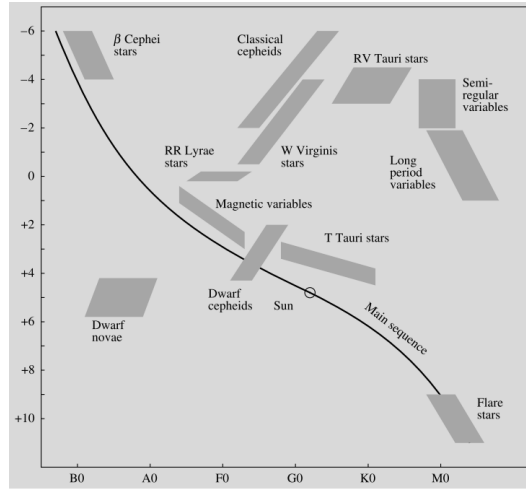


Figure 4: HR diagram showing the instability strip composed of the Classical Cepheids, W Virgins RR Lyrae stars and dwarf Cepheids. Other families of variable stars and their location on the HR diagram are also shown. Figure extracted from (4)

In addition to these main types of pulsating stars, there are other smaller but still notable classes, including the dwarf Cepheid and the  $\delta$  Scuti stars, that are fainter and their brightness varies much quicker than normal Cepheids. These stars usually have multiple periods and are more likely to have them if their amplitude variation is shorter.

In the case of  $\delta$  Scuti stars, they are located below RR Lyrae in the HR diagram (figure 4), so they cross the main sequence. This means that they are the most numerous pulsating stars (5).

A summary of some the main characteristics of pulsating variable stars are shown in table 1

Variable type	P (days)	Spectral type	$\Delta m$
Cepheids and W Virginis	de 1 a 50	F-K1	$<2$
RR Lyrae	$<1$	B8-F2 III	$<0.7$
$\delta$ Scuti	de 0.05 a 0.2	F III	$<1$
Mira variable	de 80 a 1000	M III	$>2.5$

Table 1: A list of some of the pulsating star types along with their periods, P, expressed in days, their spectral class and the variation on their magnitude  $\Delta m$ . (6)

### 1.3 Light curves. Flux and magnitudes

In order to understand the type of variable star or even to consider if a star is variable or not, it is necessary to obtain its light curve. In this section it

will be explained what exactly is a light curve and the magnitudes needed to understand how to obtain it.

Luminosity,  $L$ , is the amount of luminous energy emitted by the star per unit time (7). It is usually measured in Watts (or in erg/s). Assuming that the source radiates isotropically (equal in all directions), which happens in typical stars, at a distance  $d$  the flux,  $F$ , that will be intercepted per unit area is defined in equation 1. As it is being assumed that the medium is isotropic, the area covered will be spherical. The flux is usually measured in  $W/m^2$  (or in  $ergs/cm^2s$ ).

$$F = \frac{L}{4 * \pi * d^2} \quad (1)$$

However, a more common way of describing the brightness of a star is through its magnitude. It is essential to distinguish between apparent magnitude and absolute magnitude. Karttunen et al 2017 (4) was consulted in order to define these magnitudes. The apparent magnitude is a way of measuring the brightness of the star as seen by the observer. The apparent magnitude is then defined as:

$$m = -2.5 \log \frac{F}{F_0} \quad (2)$$

Where  $F$  is the observed flux density and  $F_0$  is the flux density for magnitude 0. Its mathematical relation with the observed flux stems from the fact that the way in which the eye perceives light is not linear but logarithmic. However, this apparent magnitude does not give the true brightness of a star, as it is related to the brightness perceived by the user. The apparent magnitude depends on the distance from the object to the observer. This is why an absolute magnitude is described, to measure the intrinsic brightness of the star. Equation 3 shows the relation between apparent magnitude and absolute magnitude. This expression is called the distance modulus.

$$m - M = 5 \log d - 5, \quad (3)$$

Where  $m$  is the apparent magnitude as describe in 2,  $M$  is the absolute magnitude and  $d$  is the distance in parsecs. The absolute magnitude would be the apparent magnitude of the object if this where to be placed at 10 parsecs from the observer.

Another important note to make is one regarding the units in which time is considered in astronomical settings. The dates regarding astronomical data are usually presented as a Julian date. This is done like this because is not dependant of an specific calendar. The Julian date number 0 is considered to be in 4713 B.C, and the number increases by one day at 12:00 UT. This means that Julian days as a unit outputs really large numbers, for example, on the noon of the first of January of 2000 the Julian date was 2.451.545 (4). This leads to modifications shifting the value of the Julian date. For example, if it were to be considered that the first of January 2000 was the day zero, that

number of Julian days would be extracted and the Julian date shifted. It is also very common to subtract 0.5 from the date to make it to coincide with the date corresponding to the Universal Time Coordinated (UTC), as it would increase one whole day at 00:00 UT instead of 12:00 UT. If the Julian date is shifted it should be specified, so if the Julian Date is referred as UTC means that 0.5 has been subtracted, and for any other kind of shifting the exact amount would be specified.

Finally, the main tool used for this project, the light curve, will be defined. A light curve is the representation of the flux or magnitude, representing the brightness of the star, in regards to time. These curves allow the user to observe how the flux of the star vary as time goes by. They can be analyse to detect exoplanets that may cross a star's path, reducing its flux and to obtain periods if the variation of the flux is periodical, leading to the possibility of classifying the stars as discussed in Sect. 1.2. However, these examples are only two of the wide variety of information that can be extracted from these curves.

Below, in figure 5 some examples of light curves from the main different types of pulsating variable discussed are shown. Also in figure 6 there is an example of an eclipsing and an eruptive stars.

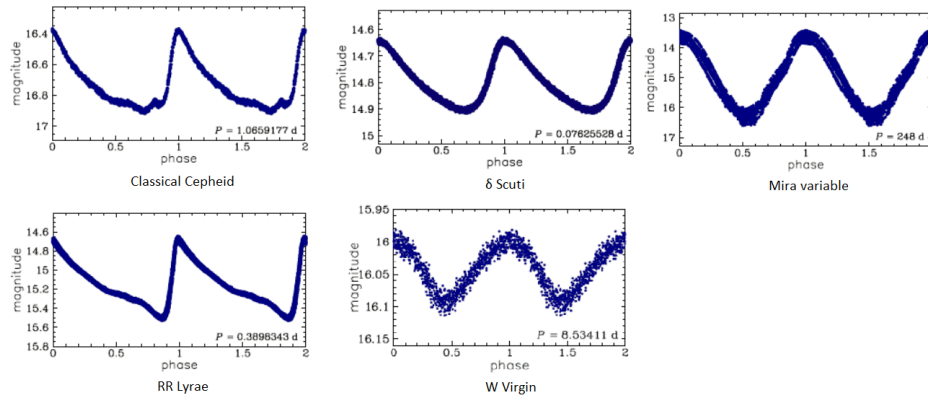


Figure 5: Light curves obtained by OGLE (8) for different types of variable stars. The magnitude is represented along time for each type, and also the period is specified.

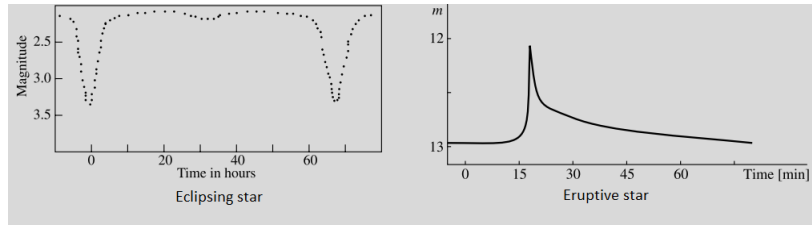


Figure 6: Example of light curves for an eclipsing star and an eruptive star. Both show the magnitude changes along time. Figure extracted from: (4)

## 2 Methods

### 2.1 Image acquisition. Astronomical observations

The first step in order to obtain the light curve is to obtain the astronomical images of our target star. The dates of observation and the telescope used are of great importance to obtain good quality images and reduce the error in the measurements.

#### 2.1.1 Visibility

In order to determine a good date it is necessary to know the equatorial coordinates of the star. These coordinates take into account the spherical geometry needed to describe the positions of celestial objects. The equatorial coordinates are defined by the projection of the Earth's equator over the celestial sphere. Just as we express coordinates on the surface of Earth with longitude and latitude, equatorial coordinates have two components: the declination,  $\delta$ , measured in degrees (from  $0^\circ$  to  $90^\circ$  to the North celestial pole and from  $0^\circ$  to  $-90^\circ$  to the South), and the right ascension  $\alpha$ , measured in hours (from 0 to 24h to the East).

The declination is the "height" of the star above the celestial Equator, so it gives important information of the latitudes at which the object can be seen from, the best being when the latitude of the observer is the same as the declination of the star ( $\phi = \delta$ ). The right ascension gives information on which times of the year the object would be visible, as it will be explained later. A graph showing these coordinates is shown in figure 7 for a better visualization of the system.

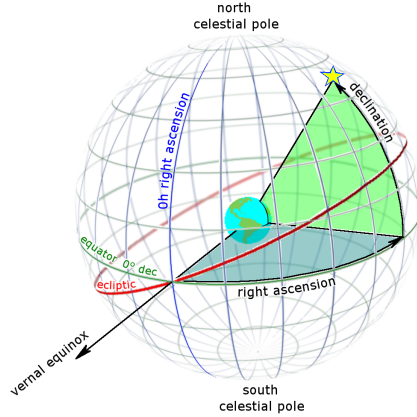


Figure 7: An scheme showing the equatorial coordinates system. The ecliptic is the apparent trajectory of the sun from Earth. Figure extracted from:(9)

It is important to introduce the concept of the hour angle, the stellar day, the sidereal day and the local sidereal time to understand how to establish a good date for observations:

-The hour angle,  $H.A.$  is the time elapsed since the star culminated, this is when the star gets to the observer's meridian, the great circle that passes through the North celestial pole, the South, and the Zenith of the observer.

-The stellar day is the time between two consecutive culminations

-The sidereal day is interval of time between two consecutive culminations of the Vernal equinox

-The local sidereal time,  $L.S.T.$ , relates the hour angle and the right ascension as follows:

$$H.A. = L.S.T. - \alpha \quad (4)$$

Furthermore, if the star is in the meridian of the observer, which are the optimal conditions for observation,  $H.A. = 0$  which means that equation 4 will be as follows for optimal observation conditions:

$$L.S.T. = \alpha \quad (5)$$

As the observations can only be done during the night, the optimal observation conditions regarding the sun's positions would be at midnight, 12 hours after its culmination:

$$L.S.T. = \alpha_s + 12^h \quad (6)$$

Where  $\alpha_s$  is the Sun's right ascension. Taken into account equations 5 and 6, the optimal right ascension for the sun would be:

$$\alpha_s = \alpha - 12^h \quad (7)$$

Knowing the optimal right ascension of the sun it is possible to establish an optimal date of observation, as this magnitude can be directly related with specific dates. For example,  $\alpha_s = 0^h$  during the Spring Equinox, on the 21<sup>st</sup> of March. The right ascension and the declination of the Sun change, as it seems to move along the ecliptic completing a revolution each year. As a full revolution would take one year, 365 days, this means that  $\alpha_s$  will take that long to get to 24<sup>h</sup>, meaning that it increases 4' per day. Using this the optimal date can be determined.

Obviously, the star can be observed other dates around this optimal date, however it won't be visible whole year round, so the closer the better. It will be considered a good day to observe if the star is visible throughout most of the night, especially around midnight when the sun's light is less likely to interfere. It is also necessary for the sky to be clear, without clouds or satellites passing by and, if possible, the location of the observatory should be on a place with little light pollution.

### 2.1.2 Instrumentation

The second important factor for the observation is the telescope as is the way of obtaining the images. There are several factors that determine whether an optical telescope is able to observe an object in a meaningful way. The most obvious one being the diameter of the telescope.

In order to establish the quality of the telescope, is important to define some magnitudes (following Karttunen et al 2017 (4)). The first magnitude its the aperture ratio,  $A_r$ , that can be defined as:

$$A_r = \frac{D}{f} \quad (8)$$

Where  $D$  is the diameter or aperture of the telescope and  $f$  the focal length. The aperture ratio is a quantity used to characterise the capability that the telescope has to gather light. If the aperture ratio is near 1, it means it is a powerful, also known as "fast", telescope. These telescopes can take photographs using short exposures. A small aperture ratio means a "slow" telescope because it needs a larger exposure time. So the larger the diameter, the better the telescope.

The second important characteristic of the telescope is the resolving power. This quantity determines the theoretical limit for the resolution of the telescope, in other words, how close two objects can be to be able to differentiate them with the telescope. It can be said that two objects can be seen separately if the angular distance between them,  $\theta$ , in radians is:

$$\theta \leq \frac{\lambda}{D} \quad (9)$$

Where  $\lambda$  is the wavelength of the light emitted by the star. This means that if the diameter of the telescope is larger, the angular distance that it can resolve is smaller, thus being able to distinguish objects more precisely.

However, the telescope is not the only instrument that will determine the resolving power. If a CCD camera is being used to take the astronomical images, this may impact the resolution, as the pixel size is important. If the pixel size is larger than  $\theta$ , then the resolution drops, as the two objects that could be separated are now on the same pixel that collects the light from the two. Nonetheless technology has advanced and now the pixel size in CCD cameras has decreased so much that it should not be a problem.

Lastly, it is important to talk about the limiting magnitude. As a star gets fainter and fainter and their apparent magnitude increases, a telescope is less likely to be able to capture the star. The limiting magnitude is the apparent magnitude threshold below which the star cannot be observed. Although this not only depends on the telescope's aperture, as the conditions of the atmosphere and the exposure time are also extremely important. However, an estimation of the limiting magnitude can be done based on the telescope's aperture, and the magnification as discussed by Schaefer, B. E. 1990 (10). A graph from this article is shown in figure 8.

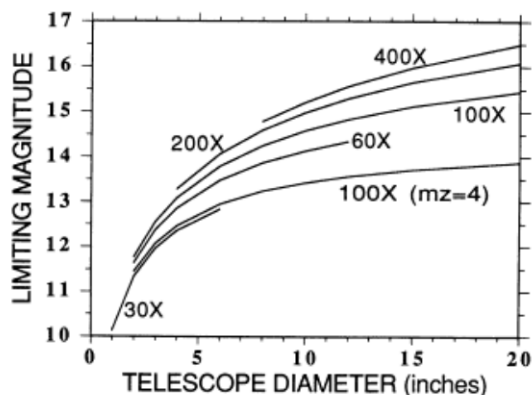


Figure 8: Representation of the limiting magnitude depending on the telescope diameter and magnification. Figure extracted from:(10)

## 2.2 Image reduction

Next step to obtain the light curve is to reduce the images. This entails getting rid of instrumental effects such as the background noise and other observational effects that naturally come with taking astronomical images. To tackle this problem and identify the main sources of error, Markus Possel, 2020(11) was consulted.

Astronomical images are usually obtained with CCD cameras. When a photon hits a pixel of the image, an electron is freed. CCD cameras are able to detect the electrons of the pixels for each row and take them to an amplifier that allows it to count the electrons. This way the number of electrons counted

should be proportional to the number of photons that have fallen into a specific pixel during the exposure time. These electrons are taken to a capacitor to measure their voltage, and this voltage can be converted into a digital number using an analog-to-digital converter (ADC), which is expressed in ADUs (analog to digital units). This digital number associated with that pixel will be higher the more light the camera has caught and lower the less light. The conversion factor between the number of electrons and this digital number is called the gain, usually expressed in  $e^-/ADU$ .

The main objective of the process of image reduction is to remove, as much as possible, all the instrumental effects so as to reconstruct the image before entering the telescope and going through the CCD camera. In order to do that it is important to understand where these effects come from (noise, the sensitivity of the pixels in the CCD camera...) and how to fix, as best as possible, these problems, mainly through the use of calibration images.

It is necessary to establish the value for zero, because even if no light falls into a certain pixel, there is still some noise. This noise corresponds with a voltage value called bias. This error is corrected by taking one or several bias frames and subtracting them from the images. A bias frame is a picture taken with the camera shutter closed and barely any exposure time, so no light is collected. That way this noise can be corrected.

The camera itself introduces some errors, specially old CCD cameras so it is necessary to obtain a dark frame. This dark frame takes into account the contribution of electrons due to electric currents caused by thermal fluctuations. Subtracting the dark frame it is possible to rectify this effect.

The last effect that is going to be corrected in this step of the process is the one due to systematic brightness distortions. This is a phenomenon produced by taking images through a telescope in which the outer parts of the image taken are darker than the centre, as clearly shown as an example in figure 9. This is expressed as having some pixels more sensitive than others, because in some parts of the CCD camera more light reaches than in others due to the experimental set up. This causes that one star from the middle of the image would appear to be brighter than other on the outer parts of the image even if that is not the case. To correct this an image is taken in which the brightness is as uniform as possible, meaning that every pixel should get the same amount of light if this effect did not happen. This image is called the flat field image, which has information about the sensitivity of each individual pixel and can be used to correct this phenomenon. Several of this images can be taken in order to get a better understanding and the error can be corrected with the master flat, that is calculated with the average of all the flat field images taken.

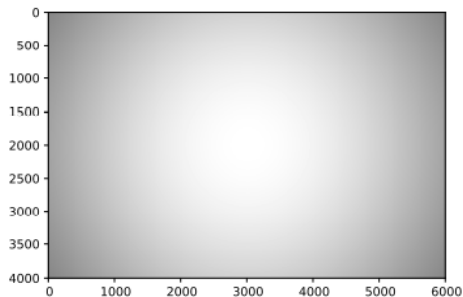


Figure 9: Flat field image taken in order to show the effect. Figure extracted from:(11)

To sum up, to reduce the images it is necessary to take extra calibration images: the bias frame, dark frame and flat field image. This way the instrumental effects can be corrected and the analysis of the images will be more accurate.

### 2.2.1 Software for image reduction

The reduction process can be done using the software AstroImageJ, an extension of the software ImageJ. ImageJ is a public domain software used for general image processing, whose capabilities can be extended to several fields of science. AstroImageJ is an extension focused on the astronomy field (12), although it keeps the image processing capabilities of ImageJ it adds a lot of tools for astronomical use such as reading FITS files, performing differential photometry and plotting light curves.

FITS or Flexible Image Transport System files are the most common for astronomical measurements. These files were created to be able to transfer astronomical image data between computers (13). This means that these files not only contain the images needed, but also important information such as the position of the images on the sky, information about the instrumentation used, the exposure time of the measurements... All this extra information is called the metadata, and is included in the FITS file alongside the measurements.

AstroImageJ is also able to subtract the bias frame and the dark frame correcting those effects. It can also create a master flat and correct this too. To do that it needs an input of the astronomical images that need to be reduced, as well as the dark, bias and flat calibration images. At the same time it is able to establish the astronomical coordinates of the image in a process called "plate solving". This is necessary because the images taken are flat, and they are in xy coordinates regarding their pixels. The FITS file usually contains information on where the telescope was pointing to while taken the measurements in equatorial coordinates so it is necessary to indicate to AstroImageJ where it can find the information on the FITS file. With this key information, AstroImageJ can convert these flat images with xy pixel counts into non-flat images in equatorial coordinates.

While this process is automated, it is necessary to manually check if all the images have been correctly processed as errors may occur. If that is the case the image can retake the process of image reduction and plate solving on its own, as doing it with only one image is less likely to cause any errors. After this process the images are ready to be analysed.

Another fact to take into account while checking if all the images have been processed correctly is to also check whether there are any visible anomalies in the images. For example, sometimes a satellite may pass by and some white stripes along the image will appear, which may cause some issues along the way. Other times the anomalies may be more subtle, so it may show later on in the light curve obtained. These may show with a larger error and a deviation from the usual pattern of the data. This defective images and data points can be deleted or omitted if the amount of images and data available are large, so a few less images will not have a great impact in the quality of the results. However, if the amount of data is little, one image less can affect the results, so it may be reasonable to take more images and obtain more data.

The reduction of images is not only important in astronomical observations, it can be used in any field that requires a photo as a means to take the measurements. Reducing the instrumental effects is necessary in all these processes.

### **2.3 Image analysis: photometry and differential photometry**

Photometry is the name of the process used to determine the apparent magnitude or flux of an astronomical object, usually from astronomical images in a range of wavelength using filters. This can be done by just adding up all of the values of the pixels that are associated with the star. However, differentiating between star pixels and non-star pixels is not as easy as it may seem at first glance. Determining when the star ends and the background begins can cause a lot of error if it is not made properly.

This problem can be solve with a method called aperture photometry, it consists on setting a circular region that contains the star and an outer annular region that only contains background as shown in figure 10 for visual aid. When summing the pixels on the region of the star it will give the light from the star plus the background. To determine the background light, the average brightness of the annular region can be determined and this average multiplied by the number of pixels in the central circle gives the value of the background light in that circle. Subtracting this background to the initial value obtained for the circle, the proper brightness of the star can be obtained.

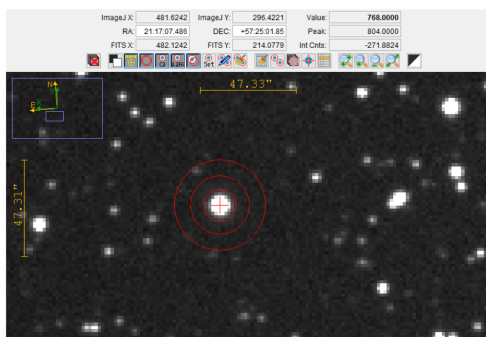


Figure 10: An example of aperture selection. The first circle would be the one defining the circular region, and the other two are defining the annular region.

However, determining the magnitude of an object accurately can be difficult. This process is called absolute photometry, and reference stars of known magnitudes and stable observing conditions are required to carry it out. This is the reason why the most common way of applying photometry, and the one used for this analysis, is differential photometry, or aperture differential photometry. This method measures the flux of a target star, in this case the variable star, relative to the flux of other comparison star. Usually more than one comparison star is used, in which case the flux of the target star is relative to the combined flux of the comparison stars. This method allows the user to properly see the variation of the brightness of one star compared with others, which is much more reliable than just measuring the brightness of a variable star with nothing to compare to as measurements taken in different nights or different settings can bring extremely different results due to the conditions of the observation. But these conditions apply to all the stars within the same image so, by comparing the target star to others in the same image, this error is reduced and measurements from different time periods can contribute to the light curve (14).

The software used for this analysis is again AstroImageJ. The way in which this software performs this multi-aperture differential photometry is as follows. First, it will perform single aperture photometry in all the selected stars. Then, the target star's relative flux is calculated by dividing the target star's integrated counts by the sum of the integrated counts of all the comparison stars. The multi-aperture allows the software to automate the task and perform this process over several images in a time series. This way it can calculate how the flux of the target star changes relative to the other stars as time goes on, and is able to display this data on a graph, obtaining a light curve. The step by step guide used for carrying out this part of the analysis is a practical meant to explain how to carry out relative photometry using AstroImageJ. This practical can be found in the web-page for a course on "Observational techniques for Astronomers" (15).

The first preparatory step to run this process in AstroImageJ is to select the comparison stars. There are several factors to take into account, as comparison

stars have a great influence on the quality and accuracy of the results. In theory the stars chosen should be just a bit brighter than the target star, however, if the target star is very dim, choosing comparison stars of similar brightness can induce unexpected errors. For example, AstroImageJ may be unable to properly find the centroid of the stars having to do it manually. In conclusion, it may result in a better outcome if the comparison stars are brighter.

Another factor to take into account is that the comparison stars can not be variable. If the comparison stars are variable, this means that the relative flux of the target star will not be accurate, as two stars are changing their brightness not only one. In order to make sure that the comparison stars are not variable two methods can be used. The first one is to check on a database, like SIMBAD (16), if the stars chosen are variable or not. Nevertheless, not all stars are in easily accessible catalogs, and that particular characteristic of the star may not be specified or maybe it is not easy to find in all catalogs. The second method, is to run multi-aperture differential photometry and see if they are variable. In order to do this, the chosen stars are run in pairs, one being the new target star and the other being the only comparison star. If the results show almost no change in the relative flux of the stars then they are not variable, however, if the light curve shows irregularities or ups and downs that star must be discarded as it probably is variable. The first method may be desirable for a star in a field where most of the stars nearby are catalogued and easily accessible in databases. The second method can be used in any circumstance, however it may be more time consuming as it can take several iterations to get to suitable stars.

Other elements that can be taken into account when choosing the comparison stars is to choose the stars that are in the centre of the field of the telescope, as that is the most sensitive area (as explain in Sect. 2.2), and it is better to avoid the outer edges of the image.

Once the comparison stars are chosen, the apertures must be placed to perform the multi-aperture differential photometry. Usually AstroImageJ will automatically find the centroid of the star chosen. However, if the star is very faint, this centroid may move away towards other nearby stars. This means that the centroid must be manually placed and it can cause some extra error. AstroImageJ has a way of helping avoid a greater error as the apertures can be placed taking into account the astronomical coordinates instead of the x-y pixel, which means that the centroids are in the same coordinates even if one of the images is slightly moved. Moreover, AstroImageJ has the capacity to align all the images just selecting some of the stars, preferably the brightest ones.

The next thing to take into account is the size of the aperture and the two radius of the annulus used to extract the background light. In order to set this values AstroImageJ has the option to "Plot Seeing Profile". An example of the seeing profile of a random star is shown in figure 11. This graph indicates the recommended values that the software is calculating for the aperture of that specific star. It is advisable to obtain the profile for different images and different days to check that the values are similar.

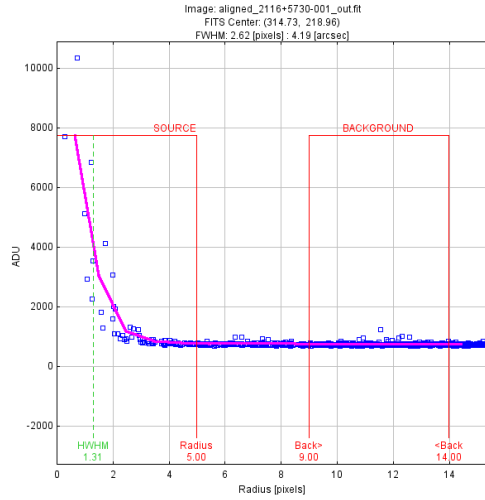


Figure 11: The seeing profile of a random star obtained with AstroImageJ (coordinates:RA=  $21^h 16' 34''$ , Dec=  $57^\circ 24' 48''$ ).

The way in which AstroImageJ chooses these values is explained by Collins et al. (12), the aperture radius is set to 1.7 times the Full Width Half Maximum (FWHM), the inner radius of the sky-background annulus is set to 1.9 times FWHM and the outer radius of the sky-background annulus is set to 2.55 the FWHM.

With all that previous steps taken into account, the differential photometry can be run, making sure that the radius of the apertures are appropriate. In order to minimize the error in the final results it can be run with several different apertures to make sure that the best one has been chosen. The values calculated can be visualise in a graph that the software displays showing the light curve and they can also be saved in different formats. It even allows to just save a few columns of data instead of all the data that this process provides to easy management of the data in other software.

AstroImageJ is also able to calculate the error of the measurements taken, as explained in Collins et al. (12). First, the software automatically calculates the total noise,  $N$ , in ADU for a CCD aperture photometry measurement, for every single aperture, as shown in equation 10.

$$N = \frac{\sqrt{GF_* + n_{pix}(1 + \frac{n_{pix}}{n_b})(GF_S + F_D + F_R^2 + G^2\sigma_f^2)}}{G} \quad (10)$$

Where  $G$  is the gain of the CCD, in electrons/ADU,  $F_*$  is the net integrated counts in the aperture in ADU subtracting the background,  $n_{pix}$  is the number of pixels in the aperture,  $n_b$  is the number of pixels in the region used to estimate sky background,  $F_S$  is the number of sky background counts per pixel in ADU,  $F_D$  is the total dark counts per pixel in electrons,  $F_R$  is read noise

in electrons/pixel/read and  $\sigma_f$  is the standard deviation of the fractional count lost to digitization in a single pixel. It is important to enter the specifications of the CCD camera used before performing the multi-aperture photometry.

Specifically, for differential photometry, the software propagates the noise from all apertures to derive the error in differential flux measurements. In order to achieve this, the noise from the apertures of each comparison star is combined as shown in equation 11 to obtain the total comparison ensemble noise.

$$N_E = \sqrt{\sum_{i=1}^n N_{C_i}^2} \quad (11)$$

Where  $N_{C_i}$  is the noise for each comparison star as calculated by equation 10, and  $n$  is the number of said stars. Then, the error is propagated through the relative flux quotient to find the relative flux error as shown in equation 12.

$$\sigma_{relflux} = \frac{F_T}{F_E} \sqrt{\frac{N_T^2}{F_T^2} + \frac{N_E^2}{F_E^2}} \quad (12)$$

Where  $F_T$  and  $F_E$  are the net integrated counts in the target aperture and the ensemble of comparison stars apertures respectively and  $N_T$  and  $N_E$  are the noise in the target star aperture and in the ensemble of comparison stars apertures calculated with equations 10 and 11 respectively.

## 2.4 Data analysis: light curve

### 2.4.1 Variability detection

Once a raw light curve is obtained, several methods can be used to determine whether variability can be significantly detected with the data available or not. In order to do this, the light curve can be adjusted to a constant. The better it fits with that constant the less it is likely to be variable. This can also be done with the non-variable comparison stars to check which one adjusts better to a constant. Several statistics can be calculated to assert whether the variable star is indeed variable. Sokolovsky et al. (17) discussed and defined several of these criteria, as they can not be applied equally depending on the circumstances. The most appropriate to use varies from case to case, as does the threshold for establishing whether the star is variable or not.

Specifically, the most important ones for this project will be the normalised  $\chi^2$  test, calculated as follows:

$$\chi_{norm}^2 = N^{-1} \sum_{i=1}^N \frac{(m_i - \bar{m})^2}{\sigma_i^2} \quad (13)$$

Where  $m_i$  is the relative flux measurement for the number of measurement taken  $i$ ,  $\sigma_i$  is its error,  $N$  is the total number of measurements taken and  $\bar{m}$  is the mean value. This test gives an idea of how well the data adjusts to the mean value. The lower this number is the better the data adjusts.

The second important statistical number would be the robust median statistic (RoMs), calculated as follows:

$$RoMS = (N - 1)^{-1} \sum_{i=1}^N \frac{|m_i - median(m_i)|}{\sigma_i} \quad (14)$$

This statistical number should have a value of around 1 when the object is not variable, and will get higher the less variable it becomes.

Finally, the Von Neumann ratio,  $\eta$ :

$$\eta = \frac{\sum_{i=1}^{N-1} (m_{i+1} - m_i)^2 / (N - 1)}{\sum_{i=1}^N (m_i - \bar{m})^2 / (N - 1)} \quad (15)$$

Usually the inverse of the Von Neumann ratio,  $1/\eta$ , is what is used to determine variability. The larger this number, the more likely it is variable.

Other statistics were considered such as the median absolute deviation (MAD), the interquartile range (IQR) or the peak to peak variability ( $\nu$ ) but they are not the best suited for this particular work according to Sokolovsky et al. (17).

#### 2.4.2 Variability characterization: Fourier analysis

Once the target star is classified as variable that shows a periodic pulse the light curve can be plotted and the analysis can start. In order to properly observe the cycle of the star, if it were to be a periodic variable star, and visualise the light curve, it is necessary to obtain its main period so it can be plotted as a function of its phase instead of the time. This way the cycle of the light curve and the shape can be easily visualise. Nonetheless, the main period is not only useful for a visual understanding of the light curve, it also gives information about the properties of the star such as the type of variable it is. However, the type of variable not only depends on the period as the shape of the curve and the variation of the magnitude are also very important.

There are several paths that can be taken to analyse the light curve and obtain its main periods but mainly most software will perform some kind of time series analysis. The type of analysis relies heavily on the type of object that is being analysed, also on the quality and quantity of the data. Time series analysis is the application of mathematical and statistical tests to quantify the variation of data along time (18).

The most important and used method is the Fourier analysis. This analysis technique uses sine and cosine functions with different periods(or frequencies), amplitudes and phases attached to them to fit the data given. This analysis allows to identify periods based on the significance of these functions calculated. The amplitudes and phases are determined with a Fourier transform, and this Fourier transform will be computed for several periods (but usually frequencies are used instead of periods) to check which ones reach a local maximum at said frequency or period.

It has several limits regarding the data. Depending on the data sets used the maximum and minimum frequencies or periods testable will change. The

minimum period (or maximum frequency) will be the time taken between measurements. The maximum frequency is related with one important parameter called the Nyquist frequency or folding frequency, and is usually half of the maximum frequency. The importance of this parameter will be discussed later on in this section. The quality of the data will affect the accuracy of the period determination, and also the minimum statistically significant amplitude, as it is necessary to differentiate between peaks due to noise and ones due to proper periods.

This analysis will output what's called a periodogram. A periodogram is a representation of the different frequencies analysed with each of them having an associated power. The higher the power, the better that period fits the data set. If there are several periods, several peaks may appear on the periodogram, showing the frequencies associated with those periods.

However, as sines and cosines are periodical functions, this means that for a set frequency, multiple periods would be possible. This is called aliasing, an effect that makes different signals seem indistinguishable from one another. This is where the Nyquist frequency can help, as this frequency defines the maximum sampling rate you need to show the full variations on the periodogram. This means that if we were to fold the periodogram in the Nyquist frequency (that is the reason why it is called folding frequency), all the aliases will meet on the same place, having now a discrete set of frequencies needed to examine all the possible periods.

Another limitation on the Fourier analysis is the noise. Every signal has noise, mainly due to the errors associated with the measurements, that will happen even with the best equipment possible. The noise level is defined as the square root of the number of photons. The Fourier analysis considers everything contained in the dataset so noise will transfer towards the periodogram. Measuring this noise, or the signal to noise ratio (SNR) is essential to determine statistical significance of a period.

The Fourier transform can be applied through different algorithms, the simplest one being the discrete Fourier transform (DFT), that as mentioned previously, just performs the Fourier transform on the data for a discrete number of frequencies. This is the base for many other Fourier methods such as the data-compensated discrete Fourier transform, the Lomb-Scargle periodogram, and Foster's CLEANest. One of the most common methods is called the Fast Fourier Transform (FFT), an algorithm invented by Gauss that reduces significantly the computation time, so it is used with really large samples of data. However, it has a big inconvenience, the data has to be evenly sampled. Moreover nowadays the computation capacity of normal computers is high enough to process the DFT based methods in a reasonable amount of time.

All these methods are discussed in greater detail by Matthew Templeton, 2004 (18).

### 2.4.3 Software for data analysis

To carry out this process the software Period04 (19) can be used. This program was developed by the TOPS (Theory and Observation of Pulsating Stars) Group, a research group based at the University of Vienna, in Austria, and the University of Texas at Austin, USA. The main focus of their work is the observation and theoretical modelling of pulsating stars that show radial and non radial oscillations. Period04 is a Java based software developed to find and fit the periodicity of these stars. It is able to import a time string, containing the 'Time', the 'Observed' and the 'Residuals to Observed'. If the data comes from AstroImageJ, the Julian date, the relative flux and its error can be introduced in Period04 for analysis.

The software allows the user to display the light curve, perform a Fourier analysis on the data, weighting the errors, display the periodogram and obtaining the frequency with the highest power. Once that frequency is obtained, the software is able to fit the data and improve the fitting pressing "improve all", this action will reduce the noise as much as possible. It will find the best fitting using the least-squares method. But it does not stop there, from this fit, another Fourier analysis can be done based on the residuals of the original periodogram. This means that the first peak detected will be "eliminated" and the Fourier analysis will give the value for the next peak. Once the second peak is obtained, the program allows the user to fit again and perform the least-square fit with both frequencies. This process can be repeated as much as the user wants, however, it is important to take the new periodograms and check visually if there were any peaks as eventually, the peaks detected will be due to noise.

Luckily, Period04 has a solution to this problem. To check whether a frequency is significant or not, it is able to obtain the SNR of a given frequency. Period considers the signal as the amplitude of the peak in the periodogram at the given frequency and the noise as the average amplitude in a given frequency range (20). The developers of the program suggest following Breger et al., 1993 (21) observational results when establishing the SNR threshold. They considered that a value for the SNR should not be lower than 4 to consider that a peak is due to the pulsation of a star and not because of the noise.

Finally, as the significant frequencies had been fitted, the software can show a graph of the light curve but this time the magnitude or flux would be represented as a function of the phase related to the period of one of the frequencies calculated, usually the main one. This the most common way of observing a light curve in order to analyse its shape, as the full cycle can be seen at a glance, including all of the data points spreaded throughout the different nights of observation. This software has a limitation here, as the light curve in phase cannot be plotted alongside the model calculated so other software may be needed for visualization.

Apart from Period04, there are several Python based packages that contain useful tools for the analysis, reduction of noise and detection of periods of a light curve. Usually low quality data lead to what's called a picket fence that appears on the periodogram. The reduction of noise to have a clearer view of

the picks on the periodogram is specially essential, as it is not an easy job with other established software. Concretely, one of the most useful packages is called "lightkurve" (22). This package contains a Light Curve class, that allows the user to import their own data with or without errors. It also has several options to remove outliers, bin the data or even fold it. It can obtain a periodogram from this light curve using different methods (such as Lomb-Scargle) and also analyse its highest peak. It also allows the user to import their own periodogram to perform noise reduction functions directly on it, the periodogram can be binned and it also has a function to smooth it. However, it is necessary to keep in mind the limitations of the data, and that these reduction of supposed noise can lead to miss important information if overdone.

Finally, VStar is a software mainly used to visualise and analyse light curves, it is mainly focused on variable star data. It was developed as part of the AAVSO's Citizen Sky project (23). It can read simple data from a text file and even from the AAVSO database directly. VStar has several options and methods to analyse and create models that adjust to the data available. This software also allows the usage of plug-ins to add on new features. For example, it may be necessary to add a plug-in, Flexible Text File Plugin, for the program to be able to read the data extracted from AstroImageJ, as the basic software is only able to read simple text format. VStar is able to work with the Julian date, the flux of the target star and its error. With the data properly inputted, the software will plot the data, and will allow to select individual points and get rid of them if necessary. Some of the data may be out of the pattern, and usually they present a higher error than other points. So this software also allows to spot this unusual points and eliminate them before analysing.

VStar uses a method called DCDFIT (date-compensated discrete Fourier transform) to obtain a periodogram. This is a type of Fourier analysis used to overcome gaps in the data, that is why it is name date-compensated, because these gaps are compensated by the algorithm (24). As other Fourier analysis methods, this process will allow the user to choose the range of frequencies and the step to obtain a periodogram representing the power for different frequencies. VStar automatically calculates and displays in a table the most powerful peaks that are more likely to be significant, which is an advantage, as it does not have to be done one by one as in Period04. Nonetheless, this can be a double edge sword as is likely that most of those peaks calculated are not significant or part of the same peak. VStar is also able to calculate a fitting model using the frequencies that the user sees adequate.

Other main advantage of VStar is that it can calculate a model based on the Fourier analysis of the frequencies inputted, and the light curve can be visualise alongside this model to check visually if it fits the data, which is a great way to observe, not only the shape of the curve, but the shape of the model's curve.

The final objective of all these programmes and software mentioned above is to obtain more information on the light curve, mainly the periods in which the brightness of the star oscillates, but also it is necessary to have a visual aid to observe the shape of the light curve in the phase representation.

## 3 Results

### 3.1 Observations

The main data used for the analysis of the light curve were obtained in the Observatorio Astronomico de Cantabria in five different nights. All of the images were obtained thanks to Javier Ruiz Fernández, an astronomer who works in the OAC whose work includes identifying variable stars. One of the initial intentions of this project was to be able to add one more set of data of another night in which the images would have been taken personally, however, due to COVID-19 restrictions it has been impossible so all the data used were the ones provided by J. Ruiz.

If the observations could have been done, it would have been necessary to prepare the visit, making sure that the star will be visible throughout most of the night or at least the hours planned for observation. Knowing the position of the observatory and the astronomical coordinates of the star is possible to check if the star will be visible for a certain date as mentioned in Sect. 2.1.

As mention before, the images used for this research were obtained using the telescope provided by the Observatorio Astronómico de Cantabria, in Valderredible whose coordinates are  $42^{\circ}46'18.0''\text{N}$   $3^{\circ}56'36.0''\text{W}$  (25). The telescope provided by the OAC has 40 cm in diameter and a CCD camera model ST-8XE/XME (26).

The variable star studied is located in ra,dec:  $21^{\text{h}} 16' 43.62''$ ,  $+57^{\circ} 24' 59.1''$ . It belongs to the constellation of Cepheus. It is a faint star and its apparent magnitude varies between 16.25 and 16.45 (27). This magnitude values mean that the telescope is being pushed to its limits, so it is necessary to be specially careful finding the centroid of the star as it is very dim. This particular star had already been preselected as a variable star using visual methods by the OAC (Javier Ruiz).

The best day for observation under those conditions was calculated as explained in Sect. 2.1. Using equation 7, it is obtained that  $\alpha_s = 9^{\text{h}}16'45''$  for the target star. Taking into account the right ascension of the Sun increases 4' per day, and knowing that when  $\alpha_s = 0^{\text{h}}$  is the Spring Equinox, the ideal date to observe the target star is 139 days after the fact, on the 7<sup>th</sup> of August.

It is also worth mentioning that the best location for the observation of the star is when the declination is equal to the latitude of the observer, so the observatory located at a latitude of around  $43^{\circ}$  and the star having a declination of around  $57^{\circ}$  is quite ideal although it would be enough just being on the same hemisphere.

Using the STARALT web-page (28), the trajectory of the star along one night selected can be plotted and visualise. As the star would have been observed in early to mid September (even though the best date was on early August), figure 12 shows the trajectory of the star on the 10<sup>th</sup> of September 2021. The star would have been easily seen throughout most of the night, including from 1am until 3am, which would have been the period of time in which the measurements would have been taken. Obviously it is necessary to take into the account the

weather conditions as well as the availability of the telescope and the position of the moon that is shown also in figure 12 as a dotted line, and it is out of the way of the star.

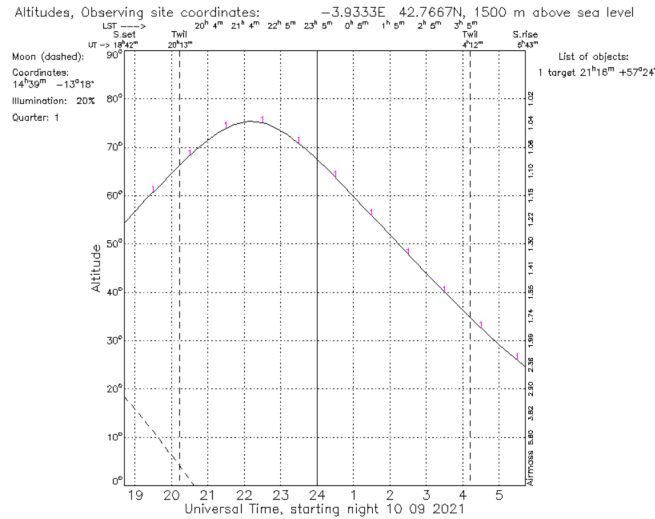


Figure 12: Trajectory of the target star on the 10<sup>th</sup> of September of 2021

Nonetheless, as mentioned previously, it was not possible to take measurements so the ones already available were used. A total of 709 images taken in 5 different nights were used, each image having an exposure time of 1 minute. The dates and number of images per night are shown in table 2. Each night bias, dark and flat field images were obtained as well as the images to analyse the star.

Date	Number of images
29-09-2011	168
18-11-2011	150
24-11-2011	25
26-11-2011	161
27-11-2011	205

Table 2: Number of images taken each date.

### 3.2 Reduction

The image reduction has been done with AstroImageJ as explained in Sect. 2.2. There are a few things to mention about the specific problems faced during the reduction process. First and foremost it is important to add specifications of the CCD camera used. These specifications can be found in the camera specifications web-page (24)

The reduction process offered by AstroImageJ was run for the five different sets of data available, and, as expected, there were some problems. In some cases the plate solving was not executed correctly so it had to be re-run but there were no major problems regarding this part of the process.

The rest of the problems arised while checking that all the images had been properly reduced. Some of the images had to be eliminated as a few white stripes appeared on them as shown in figure 13, probably due to a satellite or a plane. This is not out of the ordinary, nonetheless nine images had to be eliminated. A less expected problem appeared in one specific image that showed some stars as double, including one of the reference stars chosen. At this point, in order to avoid the error of that specific star, the reference star was changed. Even with that, the results obtained from that image were still strange, it had a greater error and the point was extremely away from the pattern of the rest of the data obtained both for the target and the comparison stars. This may have been due to one of the reference images being an eruptive star, having a sudden change in brightness. In the end that image was eliminated too.

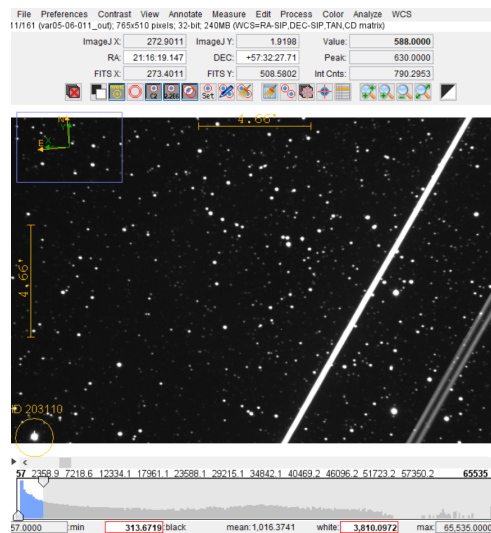


Figure 13: Astronomical image obtained that shows white stripes, probably due to a satellite or a plane.

Once the images were reduced and the plate solving was completed the next steps to analyse the data and obtaining the light curve could be taken. A comparison of the before and after of this process is shown in figure 14. It can be seen that the background is more uniform than before, there was previously a much brighter part surrounding the centre of the image, and darker spots on the outer parts and in the middle. These defects were successfully corrected in the process of reduction, as it can be seen in the image after reduction. However, it can also be seen that the process is not perfect, as the bottom left side of the

reduced images is still darker than the upper right side.

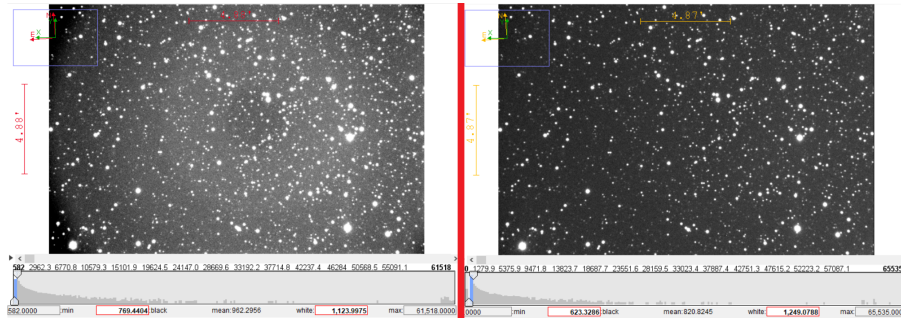


Figure 14: The image before the reduction process can be seen at the left and the one on the right is the image obtained after the reduction process has been done.

After the process of reduction and the elimination of the troublesome images, the final number of measurements used was 699.

### 3.3 Light curve extraction

#### 3.3.1 Choosing comparison stars

The first step of this part was to choose the comparison stars taking into the account the criteria explained in Sect 2.3. As mentioned there, the stars chosen should be just a bit brighter than the target star, however, the target star studied in this case is very dim. It needs to be taken into account that, due to the size of the telescope used, this star is near the limit of what it can observe, so it is being pushed to its limits. This means choosing comparison stars of similar brightnesses can induce unexpected errors. No filters were used in our observations in order to capture as much light as possible. Setting a filter is reducing the amount of total light that can reach the telescope. Even with that, in this case the star was so dim that AstroImageJ had a hard time finding the centroid and it had to be done manually in some cases. After several tries results showed that it was better to choose slightly brighter stars to get a more accurate result.

The second key factor was that the comparison stars cannot be variable. In order to make sure of that, two methods were explained in Sect 2.3, one in which a database has to be checked to make sure that the comparison stars are not variable. Nevertheless, the observed field could not be chosen and there was not a lot of information on the stars that had an appropriate apparent magnitude to use as comparison stars. Because of that, the second method was used, in which the comparison stars were analysed with differential photometry on pairs to check that their brightness did not vary. Figure 15 shows the light curve obtained with AstroImageJ on the night of 18<sup>th</sup> of November of 2011 for all of

the comparison stars chosen (although the process to determine whether they were constant was made in pairs). As it can be seen the light curve is almost constant.

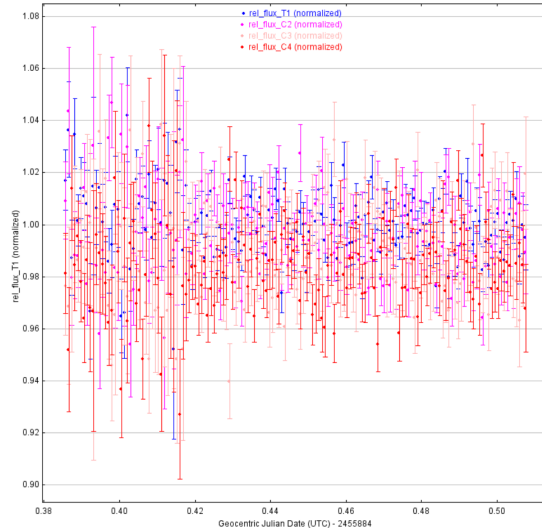


Figure 15: Light curve obtained with AstroImageJ for the comparison stars. The plot shows the relative fluxes of the stars as a function of the time expressed in UTC.

Through a method of trial and error with different comparison stars of different magnitudes, the final amount of stars chosen is four. The astronomical coordinates of these comparison stars are shown in table 3, and a photograph with all of the stars marked is shown in figure 16

	RA	dec
C2	$21^h 16' 46''$	$57^{\circ} 24' 59''$
C3	$21^h 16' 37''$	$57^{\circ} 25' 07''$
C4	$21^h 16' 34''$	$57^{\circ} 26' 14''$
C5	$21^h 16' 36''$	$57^{\circ} 26' 37''$

Table 3: Comparison stars coordinates

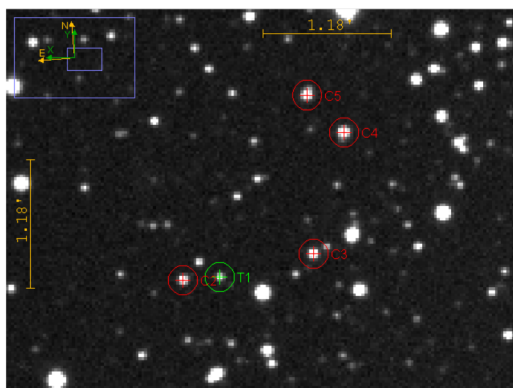


Figure 16: One of the images taken on the 18th of November of 2011 where all the comparison stars:  $C2$ ,  $C3$ ,  $C4$  and  $C5$ , as well as the target star  $T1$ , are shown.

Through this process of trial and error, another possible variable star was identified while comparing the potential comparison stars. Figure 17 shows the light curve of that star ( $T1$ ) during the night of 26/11/2011. It was an interesting discovery as this behaviour was not observed every night, so every comparison star had to be rechecked making sure it was non variable every night.

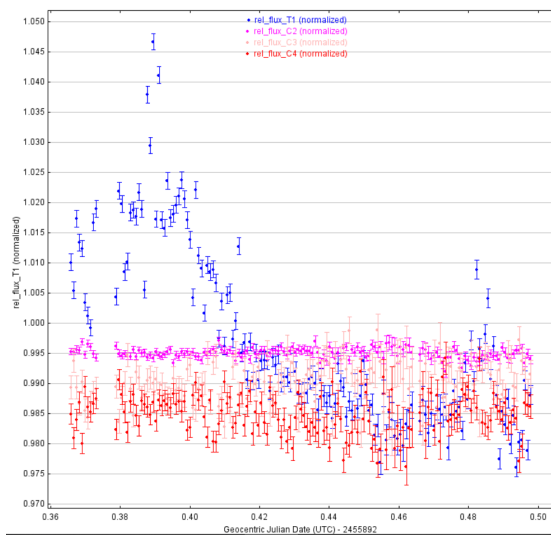


Figure 17: Rough light curve of an possible variable star ( $T1$ ) located at RA: $21^h16^m55^s$ , dec: $57^{\circ}24'11''$  obtained with AstroImageJ. The plot shows the relative fluxes of the stars as a function of the time expressed in UTC.

### 3.3.2 Differential photometry

Once the comparison stars were chosen, all the data sets were to be run through the process of multi-aperture differential photometry in AstroImageJ. However, the parameters of the aperture had to be chosen. As discussed in Sect. 2.3, AstroImageJ has the option "Plot seeing profile". The one obtained for the target star is shown in figure 18. This was a difficult process, the star is so dim that, as mentioned previously, AstroImageJ has a hard time identifying the centroid so it was necessary to set it manually. As it can be seen, this fact made it a harder for AstroImageJ to calculate the values as it does not have a distinct profile unlike brighter stars, that have a sharper peak like the one showed in figure 11. Moreover, the target star has other stars really nearby, so the background has a lot of noise from those stars, that can be avoided choosing an smaller aperture. This may lead to errors so it is advisable to run the multi-aperture differential photometry with different apertures on the different stars (not only the target star) that will be used to check if the values obtained for the aperture are reasonable. Furthermore, several seeing profiles were taken for different days and different stars to compare the results, and finally the values used were 5 for the radius and 9 and 14 for the background.

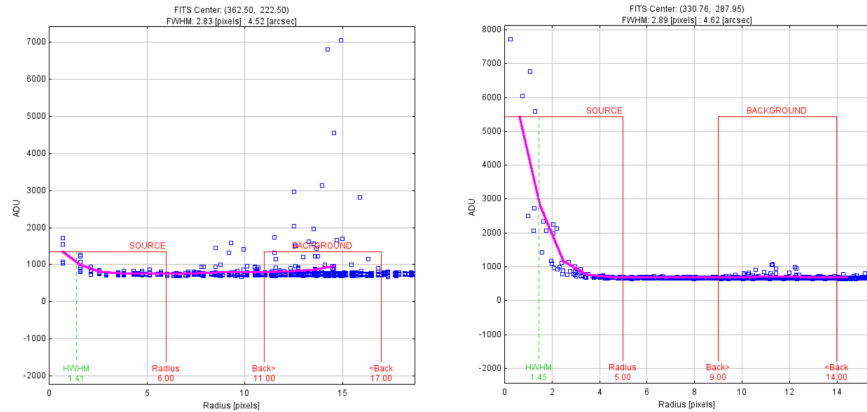


Figure 18: At the left, the seeing profile obtained by AstroImageJ for the target star. At the right the seeing profile of one of the comparison stars (C4) that shows the aperture parameters used.

All the options for the aperture settings are shown in figure 19 along with the CCD camera specifications.

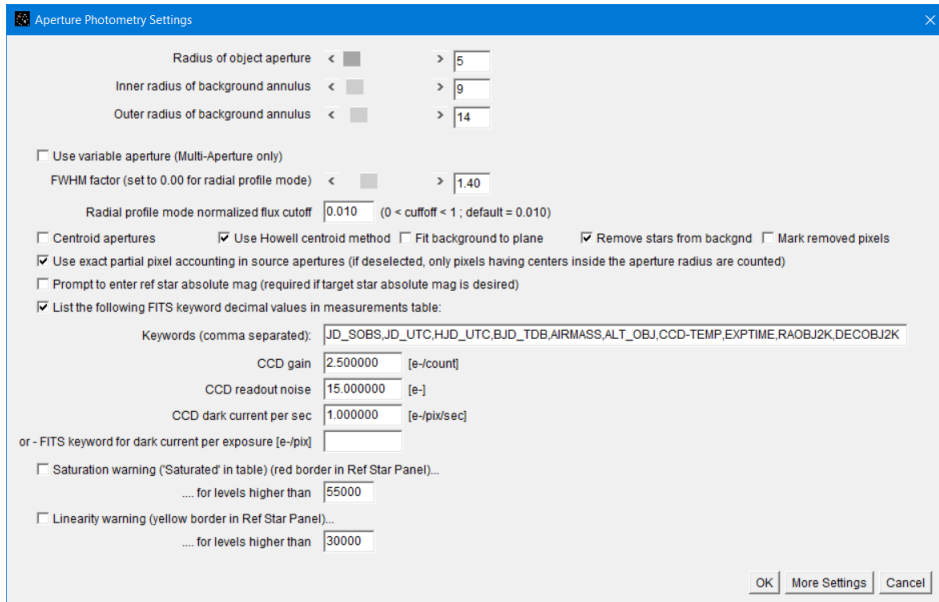


Figure 19: Aperture settings displayed by AstroImageJ, including the extra settings for the CCD camera.

The final step is running the multi-aperture differential photometry in all the data sets available obtaining a rough light curve. As the observations were made in five different days, there are a total of five different data sets. All of the data obtained from each individual data set was saved, and later on merged into one file to obtain a single light curve to analysed. An example of the graph plotted by AstroImageJ for the data obtained on the 18<sup>th</sup> of November of 2011 is shown in figure 20.

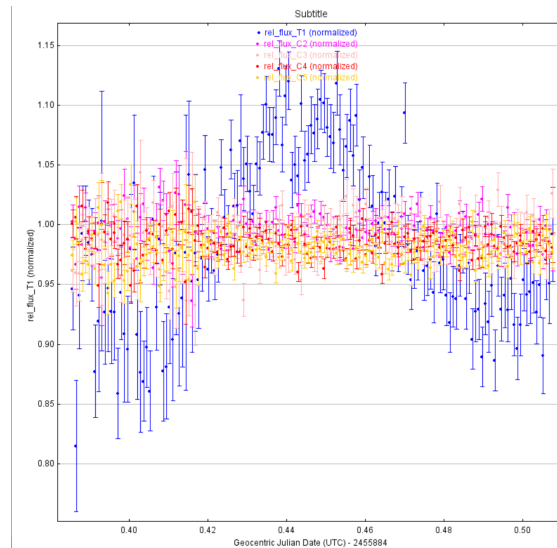


Figure 20: An example of a graph obtained for the target star's light curve through AstroImageJ. The plot shows the relative fluxes of the stars as a function of the time expressed in UTC.

### 3.3.3 Variability detection

With all the data compiled in one file the process of analysis is ready to begin. The first step was to assess whether the target star was variable taking into account the error in the measurements calculated by AstroImageJ. In order to do that the light curve of all the stars used is adjusted to a constant. The more it fits the less variable it would be. A graphic representation of this is shown in figure 21. The relative flux is represented regarding the measurement number instead of the time due to the fact that, when represented in relation to time, the data points would not be clearly visible as the dates of observation are spread throughout several months. A zoom on the target star is done and it already seems to be variable at a first glance.

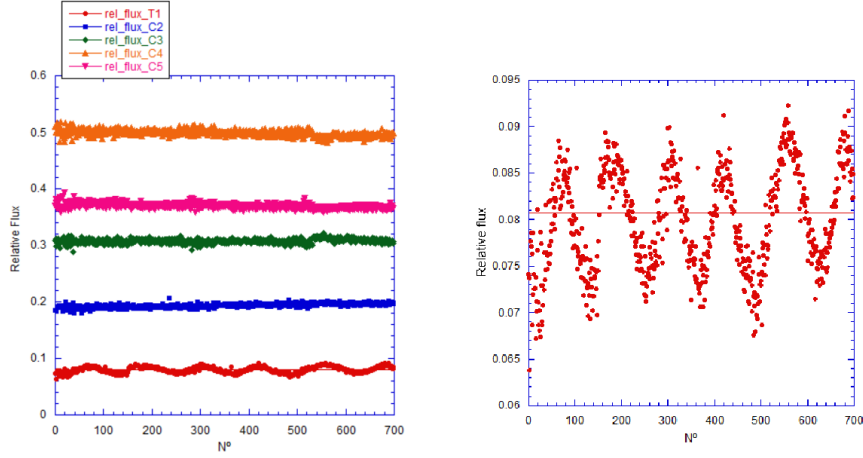


Figure 21: Representation of the relative flux of all the stars relative to the measurement number. At the right it can be seen a zoom on the target star T1

To establish whether the data fits a constant or not, several of the statistical numbers described by Sokolovsky et al. (17) are calculated for the target star as well as the comparison stars. The results obtained are shown in table 4

	$\chi^2$	$\chi^2_{norm}$	$MAD$	$IQR$	$RoMS$	$v$	$1/\eta$
T1	6896,70000	9,86660	0,00440	0,0089	2,69750	0,14330	3,65230
C2	1753,10000	2,50810	0,00260	0,0052	1,28270	0,05570	0,97144
C3	1285,30000	1,83880	0,00250	0,0051	1,08880	0,03810	0,69449
C4	1439,10000	2,05890	0,00370	0,0075	1,15140	0,02500	0,72748
C5	1195,60000	1,71040	0,00260	0,0053	1,04830	0,03330	0,68376

Table 4: Statistical numbers calculated for the target star ( $T1$ ) and all of the comparison stars ( $C2-C5$ ), that show how closely their light curves fit with a constant.  $\chi^2$  is the  $\chi^2$  test result and  $\chi^2_{norm}$  is that number normalised to the number of data points.  $MAD$  is the median absolute deviation,  $IQR$  is the interquartile range,  $RoMS$  is the robust median statistic,  $v$  is the peak to peak variability, and  $1/\eta$  is the inverse of the Von Neumann ratio.

The difference for the target star  $T1$  and all of the comparison stars is noticeable. To establish the threshold, for which this difference would be significant, other articles were explored. It was established that the threshold for the  $\chi^2$  normalised would be that the variable stars would have a value larger than 3 (29) if and when the data has larger errors. For the robust median statistic ( $RoMs$ ) the established threshold was 2.5 and 1.4 for the inverse of the Von Neumann ratio ( $1/\eta$ ) (30). The target star not only fits all these parameters, but both the peak to peak variability,  $v$ , and the median absolute deviation,  $MAD$ , are noticeably higher for the target star when compared to the constant

stars. With all this information it can be deduced that the target star is in fact variable, moreover, based on its light curve shown in figure 21, it seems that it may be a periodic variable. The methods described in 2.4 were used to obtain this period, as it is explained in Sect. 3.4.

### 3.4 Light curve analysis

As the star being analysed seems to follow a periodic variation, the two main objectives of this part of the process will be to obtain the main period of the target star and the type of variable star. As discussed in Sect. 2.4 there are several methods to obtain this period.

The software Period04 was used to obtain the periodogram and also to estimate the significance of the peaks. The light curve obtained with AstroImageJ was inserted in this software as a time string. Period04 automatically calculates the Nyquist frequency obtaining a value of 607.59 cycles/day.

Then, the Fourier analysis was carried out, from frequency 0 till the Nyquist frequency (rounded). The errors calculated by AstroImageJ were taken into account. The first periodogram obtained with Period04 is shown in figure 22. As it can be seen when zoomed (figure 23), there are a few visible peaks but there is a lot of noise in the periodogram and that needs to be worked on.

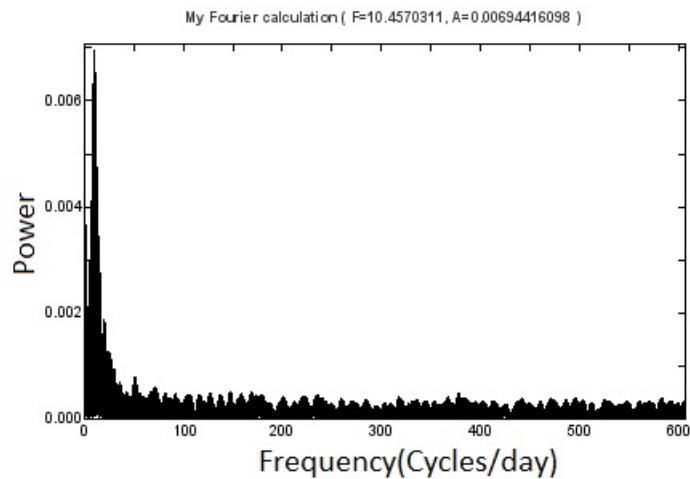


Figure 22: Complete periodogram for the light curve.

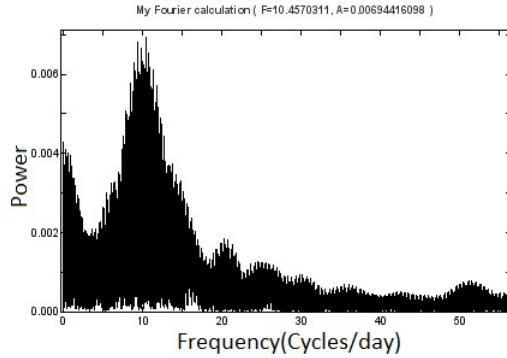


Figure 23: Zoomed periodogram for the light curve.

Using an external program, coded with the Python extension 'lightkurve', this periodogram was imported to be refined. The periodogram was binned using the 'median' method and a bin size of 50. Figure 25 shows the final periodogram obtained after the refinement, a big difference can be appreciated comparing with the previous one (figure 22). Nonetheless both peaks are still visible and in the same position. The main peak was at a frequency of  $f_1 = 10.34$ cycles/day and after the refinement, the peak was at  $f_2 = 10.45$ cycles/day

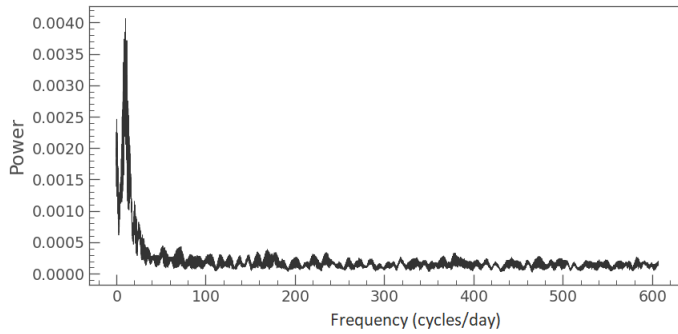


Figure 24: Periodogram obtained for the light curve after the smoothing process of lightkurve.

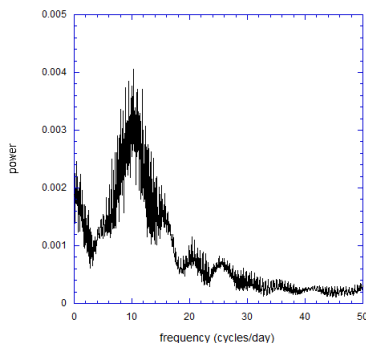


Figure 25: Zoomed periodogram obtained for the light curve after the refinement process of lightkurve.

Period04 identifies multiple peaks on the periodogram but except for two of them, their SNR is below the appropriate threshold of 4 (21) to consider them significant. The important data regarding those peaks is shown in table 5.

Frequency(1/d)	Period(d)	SNR
10.457	0.095	24.45182
0.051	19.607	9.63338
7.369	0.135	3.05733
20.398	0.049	2.98131

Table 5: Main peaks detected by Period04 and their SNR.

It appears to be two peaks that are statistically significant, and their SNR are notably larger than the rest of the peaks. These candidates that are detected due to noise may be an alias, or near an alias of the two main peaks. For example, 20.39 c/d is roughly double of the main frequency 10.45 c/d.

There is more discussion that can be made as the second peak arises some questions. Is it truly a peak showing the period of the star or a peak due to the spacing on the measurements taken? It was discussed in Sect. 2.4 how the periodogram is obtained, and how it tries to fit the function with periodic functions. This can lead to significant peaks due to other factors than the periodic brightness of the star. For examples if measurements were taken every night at the same time, a Fourier analysis would show a significant peak at a period of 1 day. In this case the second peak,  $P=20d$ , is likely due to the time separation between the measurements of the first and the rest of the different nights. This suspicion was cleared when another periodogram was obtained omitting the first day's measurements because this night was 19 days apart from the next one. So that would be the cause of error. Performing the same analysis, the first peak of  $P=0.095$  appeared as expected, however, the second peak with a period of approximately 20 days did not appear, instead, the second

peak had a period of 0.3 days approximately.

Due to all of the points discussed above, the fitting will be carried out using only the first frequency, that has a period of  $P=0.095d$  and an adjusted phase of  $ph=0.427862$ .

A way of checking if the data is being properly fitted is by checking visually if the model is adjusting to the data. However, with Period 04 it can only be done in the normal time string and not in the phase light curve. Figure 26 shows how the model calculated fits the data of one of the nights.

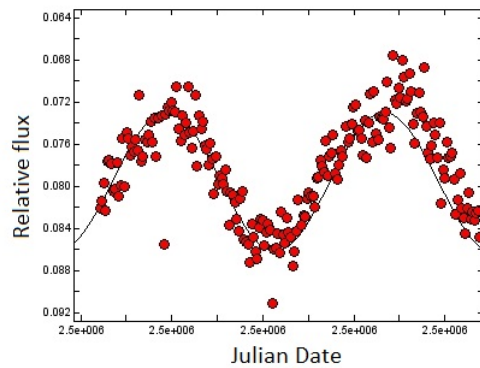


Figure 26: Light curve and the model calculated by Period04, but only the data from one night can be seen. The red dots are the experimental data and the black line the model fitted by Period04

Finally, figure 27 shows the light curve in phase, based on the first and most significant period,  $P=0.095d$ . Most of the data follows the same pattern and a clear shape is defined. However, a better visualization of the data and the model that fits it can be done with VStar.

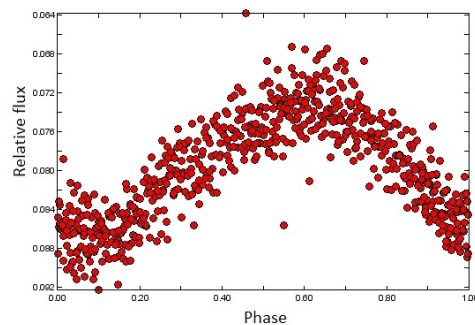


Figure 27: Light curve in phase taking into account the fundamental frequency as  $f=10.45$  cycles/day

Knowing the significant peaks, the light curve was introduced in VStar for visual aid, nonetheless, it was necessary to carry out an analysis using this software to get the desired graph, so it is also a great opportunity to compare the results. The plug-in Flexible Text format had to be used, so the program could read the AstroImageJ file just by altering the headings. A periodogram was obtained using the method DCDFt explained in Sect. 2.4, it was calculated for frequencies between 0 and the Nyquist frequency obtained by Period04. This periodogram is shown in figure 28. In figure 29 a zoom of the periodogram can be seen with the peaks that VStar considers relevant.

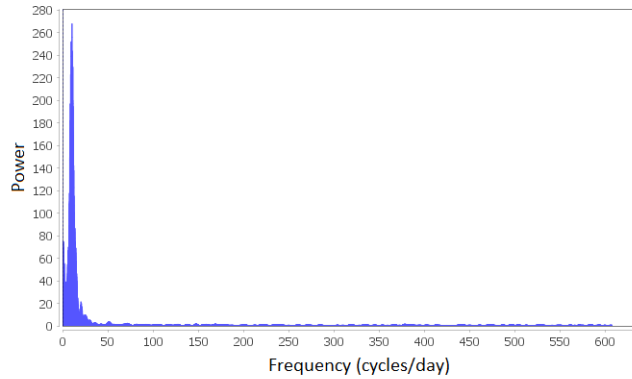


Figure 28: Periodogram obtained with the software VStar.

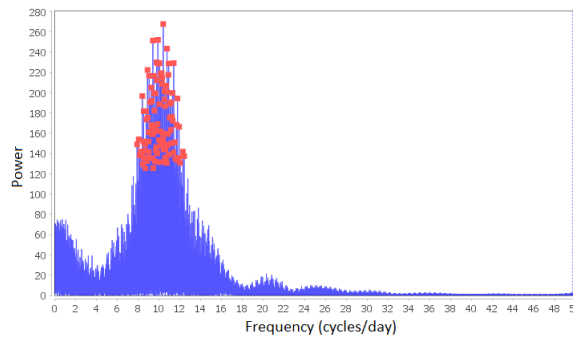


Figure 29: Zoomed periodogram obtained with the software VStar. The red dots show the peaks that VStar considers significant.

The highest peak obtained is the same as the one obtained with Period04

as it was expected, however, the rest of the "peaks" detected are ones that Period04 considered the same peak. VStar has a way around this problem. As in Period04, you can fit the data, and recalculate another periodogram based on the residuals, that being, removing the main peak. This new periodogram is shown in figure 30. However, there is a problem similar to that of Period04, the period corresponding with this peak is around  $P=1.3$  days, which is probably another detection of the spacing on the last 3 nights of measurements. A periodogram using only the measurements of the first two days was analysed because they are 19 days apart, so if this peak is due to the measurements spacing the peak should not appear. The first peak that appears in this new analysis is the expected one,  $P=0.095$  days, however, the second peak that appears is  $P=0.629$  days. So is highly likely that the previous peak detected by VStar was due to the spacings of measurements.

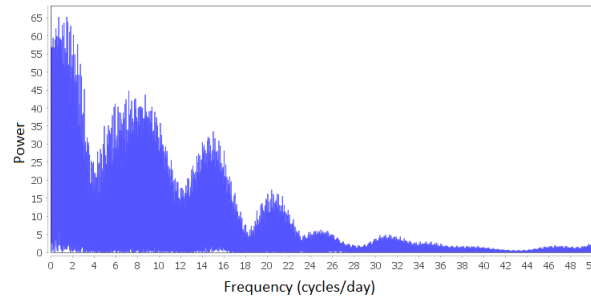


Figure 30: Second periodogram obtained with the software VStar zoomed for seeing better the peaks.

In summary, after this analysis the only really significant period detected by both software was  $P=0.095$  days, the fit that is obtained using this peak, and its phase, is quite accurate, as it is shown in figure 31. As it happened with the light curve in Period04, there are some outliers, but it can be seen that most of them show larger errors than most of the data, so they are probably due to the low quality data for the corresponding images. Unlike Period04, VStar shows two complete cycles of the star so it is easier to visualise and compare, later on, with other light curves.

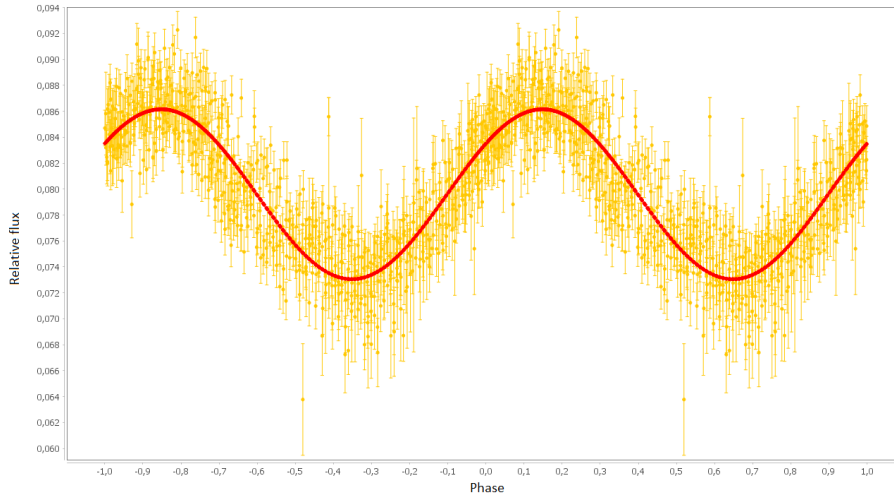


Figure 31: Light curve in phase. The yellow dots are the measurements with their error bars and the red line is the model calculated by VStar with the main period  $P=0.095d$ .

Vstar is able to output the function equation of the model calculated:

$$f(t) = 0.079592 + 0.005233\cos(2\pi 10.45697(t - zP)) - 0.004062\sin(2\pi 10.45697(t - zP))$$

Where  $zP$  is the 'zeroPoint' in this case  $zP=2455885,7$  days.

It can be seen that the data seems to follow the model calculated quite well once again, implying that the period detected is in fact significant. Finally, in figure 32 the light curve can be seen again plotted with the residuals (data minus model).

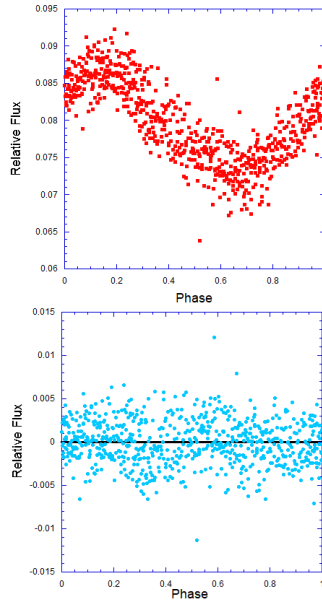


Figure 32: Light curve in phase (for a period of 0.095 days) with the residuals. The red dots at the top are the measurements and the blue dots at the bottom are the residuals. The zero line is also plotted as a black line so it can be seen how much the residuals deviate from it.

## 4 Discussion

Based on the light curve, the main period of the star was obtained  $P=0.095d$ . Other secondary peaks were detected as well, although not all them with a SNR high enough to be considered significant. Besides, not all secondary peaks showed in the two analysis using two different software (Period04 and VStar). Moreover, further analysis of some of those peaks strongly implied that they were cause by the time spacing between the different nights in which the data were collected, instead of the variability cycle of the star.

Being conservative, just the first main period and the magnitude variation were used to discuss what type of variable star it is, but we may take into account that it may contain a secondary or more periods that could not be properly detected due to instrumental effects and the faintness of the star.

To begin with, it has a really short main period, so it experiences extremely rapid changes. Referring back to table 1 in Sect. 1.2 this is a clear characteristic of a  $\delta$  Scuti star. Moreover, taking the highest relative flux value of the light curve,  $relF_{max}=0.092$ , and the lowest,  $relF_{min}=0.063$ , the amplitude variation is  $\Delta relF = 0.02$ . Using equation 2, this relative flux variation equals to a difference in apparent magnitude of around 0.9 which is also in accordance with what was discussed about  $\delta$  Scuti stars. Specifically, when  $\delta$  Scuti stars have a

higher magnitude variation than 0.3, they are considered high-amplitude  $\delta$  Scuti (HADS)(8). These stars usually only have one mode of pulsation, in contrast to variables with smaller amplitudes who are known to have more than one mode of vibration. HADS usually have really similar curves of those of Cepheids, that is why they are sometimes referred to as dwarf Cepheids, with the main difference being the shorter periods and smaller magnitude changes. HADS are usually in the final hydrogen burning stage of their life (5), meaning they are about to leave the main sequence and enter the giant phase.

Finally, another important factor to determine whether this star is a  $\delta$  Scuti or not, is the shape of the curve. One example was shown in figure 5 back in Sect. 1.3. It seems like the curve in that figure is more rounded and is obviously more clear than the one being analysed here (figure 31). However, looking at other sources like the OAC (31), they show this example (figure 33) of a  $\delta$  Scuti detected with the same equipment this analysis used.

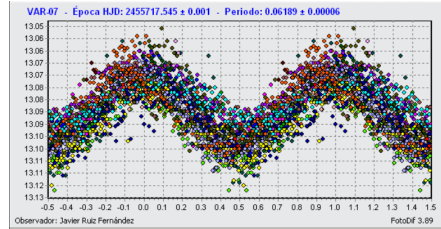


Figure 33: Light curve in phase of a  $\delta$  Scuti star discovered by the OAC (31)

There are clear similarities between this curve and the one obtained. Moreover, going back to the source of the other pulsating variables light curves, OGLE (8), they have way more examples of  $\delta$  Scuti stars, the most similar to the one being discussed are shown in figure 34

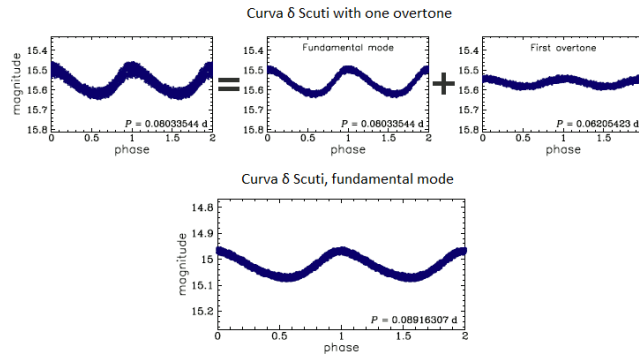


Figure 34: Light curve of different  $\delta$  Scuti stars obtained by OGLE (8), the upper one shows the light curve, as well as its main pulsation mode and the first overtone and the bottom one shows the just usual light curve

All this evidence strongly suggest that the star analysed is indeed a  $\delta$  Scuti star, specifically a HADS. To remember what was explained about this stars in Sect 1.2,  $\delta$  Scuti stars are in the same instability strip as Cepheids, but the main difference is that they are fainter and have shorter periods of pulsation, which is what happens with this particular star. They also follow a similar period to luminosity ratio as Cepheids, which means it could be possible to determine the distance at which the HADS is, however, in order to do this, it would have been necessary to perform absolute photometry in different filters, and this is not our case.

## 5 Conclusions

Based on all the information presented, it can be concluded with a high certainty that the star analysed is a  $\delta$  Scuti star. However, getting to this conclusion is not as straight forward as it may seem.

Working with real data and all that it involves is not an easy task. Moreover, due to the faintness of the star it was even more important to treat these data with caution to be able to get accurate results. The astronomical images were reduced as to mitigate the instrumental effects as much as possible. With this reduces images the light curve of the target star was extracted and, through the study of the data with some statistics, it was determined that the star studied was variable. Not only that but it showed that this variability could be periodic.

A further analysis was carried out to obtain the main period of the star and prove that the variability was periodic. Using different methods with different software it was determined that the fundamental frequency was 10.45 cycles per day, that is equivalent to 0.095 days. This short period already suggest that this star is a  $\delta$  Scuti star, and its magnitude variation and the shape of the curve also back this possibility. More specifically, due to the amplitude of its magnitude variation, this star was classified as a High-Amplitude  $\delta$  Scuti star.

## 6 Bibliography

### References

- [1] Robert Hollow. The hertzsprung-russell diagram. *Australia Telescope National Facility, CSIRO*. URL [https://www.atnf.csiro.au/outreach/education/senior/astrophysics/stellarevolution\\_hrintro.html](https://www.atnf.csiro.au/outreach/education/senior/astrophysics/stellarevolution_hrintro.html).
- [2] Khodayar Taghinyarami. *Rotational Evolution of Low-Mass stars in close binaries*. PhD thesis, 07 2016.
- [3] Michael Wiescher. Cosmic alchemy in the laboratory. *Physics*, 2, 08 2009.
- [4] Hannu Karttunen. *Fundamental Astronomy*. Springer Heidelberg, 2017. ISBN 978-3-662-53044-3.

- [5] John R. Percy. *Understanding variable stars*. Cambridge University, 2007. ISBN 978-0-511-28514-1.
- [6] Mónica Fernández Perea. Curvas de luz de estrellas variables. September 2002. URL <http://webs.ucm.es/info/Astrof/users/jaz/TRABAJOS/VARIABLES/variables01.html>.
- [7] Neil de Grasse Tyson, Charles Liu, and Robert Irion. Flux, luminosity and the inverse square law. URL [https://www.nap.edu/resource/oneuniverse/energy\\_knowledge\\_concept\\_7.html](https://www.nap.edu/resource/oneuniverse/energy_knowledge_concept_7.html).
- [8] Andrzej Jarosław Udalski. Ogle atlas of variable star light curves. URL <http://ogle.astrouw.edu.pl/atlas/index.html>.
- [9] Wikipedia. Right ascension. URL [https://en.wikipedia.org/wiki/Right\\_ascension](https://en.wikipedia.org/wiki/Right_ascension).
- [10] Bradley E. Schaefer. Telescopic Limiting Magnitudes. *Publications of the Astronomical Society of the Pacific*, 102:212, February 1990.
- [11] Markus Pössel. A beginner’s guide to working with astronomical data. *The Open Journal of Astrophysics*, 3(1), Jan 2020. ISSN 2565-6120. URL <http://dx.doi.org/10.21105/astro.1905.13189>.
- [12] Karen A. Collins, John F. Kielkopf, Keivan G. Stassun, and Frederic V. Hessman. AstroImageJ: Image processing and photometric extraction for ultra-precise astronomical light curves. *The Astronomical Journal*, 153(2): 77, jan 2017. URL <https://doi.org/10.3847/1538-3881/153/2/77>.
- [13] R. J. Hanisch, A. Farris, E. W. Greisen, W. D. Pence, B. M. Schlesinger, P. J. Teuben, R. W. Thompson, , and A. Warnock III. Definition of the flexible image transport system (fits). *Astronomy & Astrophysics*, 2001. URL <http://www.cv.nrao.edu/fits/aah2901.pdf>.
- [14] J. L. Sokoloski, Lars Bildsten, and Wynn C. G. Ho. A search for rapid photometric variability in symbiotic binaries. *Monthly Notices of the Royal Astronomical Society*, 326(2):553–577, 09 2001. ISSN 0035-8711. URL <https://doi.org/10.1046/j.1365-8711.2001.04582.x>.
- [15] Observational techniques for astronomers: P03 photometry practical. URL <http://slittlefair.staff.shef.ac.uk/teaching/phy217/lectures/principles/L03/index.html>.
- [16] Simbad, astronomical database. URL <http://simbad.u-strasbg.fr/simbad/>.
- [17] K. V. Sokolovsky, P. Gavras, A. Karamelas, S. V. Antipin, I. Bellas-Velidis, P. Benni, A. Z. Bonanos, A. Y. Burdanov, S. Derlopa, D. Hatzidimitriou, A. D. Khokhryakova, D. M. Kolesnikova, S. A. Korotkiy, E. G. Lapukhin, M. I. Moretti, A. A. Popov, E. Pouliasis, N. N. Samus, Z. Spetsieri,

- S. A. Veselkov, K. V. Volkov, M. Yang, and A. M. Zubareva. Comparative performance of selected variability detection techniques in photometric time series data. *Monthly Notices of the Royal Astronomical Society*, 464 (1):274–292, 09 2016. ISSN 0035-8711. URL <https://doi.org/10.1093/mnras/stw2262>.
- [18] Matthew Templeton. Time series tutorial. *Journal of the AAVSO*, 32(1): 41, 2004. URL <https://www.aavso.org/time-series-tutorial>.
- [19] Michel Breger. The tops group website. URL <https://www.univie.ac.at/tops/>.
- [20] P. Lenz and M. Breger. Period04 user guide. *Communications in Asteroseismology*, 146, jun 2005. URL <https://ui.adsabs.harvard.edu/abs/2005CoAst.146...53L>.
- [21] M Breger, J Stich, R Garrido, B Martin, SY Jiang, Zhi-ping Li, DP Hube, W Ostermann, M Paparo, and M Scheck. Nonradial pulsation of the delta-scuti star bu-cancri in the praesepe cluster. *Astronomy and Astrophysics*, 271:482, 1993.
- [22] Lightkurve Collaboration, J. V. d. M. Cardoso, C. Hedges, M. Gully-Santiago, N. Saunders, A. M. Cody, T. Barclay, O. Hall, S. Sagar, E. Turtelboom, J. Zhang, A. Tzanidakis, K. Mighell, J. Coughlin, K. Bell, Z. Berta-Thompson, P. Williams, J. Dotson, and G. Barentsen. Lightkurve: Kepler and TESS time series analysis in Python. Astrophysics Source Code Library, December 2018.
- [23] Vstar page in the aavso website. URL <https://www.aavso.org/vstar>.
- [24] David Benn. Vstar user manual. URL <https://www.aavso.org/sites/default/files/vstar/VStarUserManual.pdf>.
- [25] Observatorio astronómico de cantabria. URL <http://max.ifca.unican.es/OAC/>.
- [26] Camera specifications. URL <http://www.company7.com/library/sbig/sbwhtmls/st8.htm>.
- [27] Target variable star’s characteristics. URL <https://www.aavso.org/vsx/index.php?view=detail.top&oid=270922>.
- [28] Staralt, object visibility. URL <http://catserver.ing.iac.es/staralt/index.php>.
- [29] Bonanos, A. Z., Yang, M., Sokolovsky, K. V., Gavras, P., Hatzidimitriou, D., Bellas-Velidis, I., Kakalettris, G., Lennon, D. J., Nota, A., White, R. L., Whitmore, B. C., Anastasiou, K. A., Arévalo, M., Arviset, C., Baines, D., Budavari, T., Charmandaris, V., Chatzichristodoulou, C., Dimas, E., Durán, J., Georgantopoulos, I., Karamelas, A., Laskaris, N., Lianou, S.,

- Livanis, A., Lubow, S., Manouras, G., Moretti, M. I., Paraskeva, E., Poulia-  
sis, E., Rest, A., Salgado, J., Sonnentrucker, P., Z. T. Spetsieri, P. Taylor,  
and K. Tsinganos. The hubble catalog of variables (hcv). *A&A*, 630:A92,  
2019. URL <https://doi.org/10.1051/0004-6361/201936026>.
- [30] A. N. Heinze, J. L. Tonry, L. Denneau, H. Flewelling, B. Stalder, A. Rest,  
K. W. Smith, S. J. Smartt, and H. Weiland. A first catalog of variable stars  
measured by the asteroid terrestrial-impact last alert system (ATLAS). *The  
Astronomical Journal*, 156(5):241, nov 2018. URL <https://doi.org/10.3847/1538-3881/aae47f>.
- [31] Javier Ruiz Fernández. Nuevas variables, 2013. URL <http://max.ifca.unican.es/OAC/>.